Controlling morphology, adhesion and electrochromic behavior of PEDOT films through molecular design and processing

*Christina J. Kousseff, Fani Eirini Taifakou, William G. Neal, Matteo Palma, Christian B. Nielsen**

C. J. Kousseff, W. G. Neal, Dr. M. Palma, Dr. C. B. Nielsen

Department of Chemistry, Queen Mary University of London, London, E1 4NS, United Kingdom

E-mail: c.b.nielsen@qmul.ac.uk

F. E. Taifakou

Department of Physics, Queen Mary University of London, London E1 4NS, United Kingdom

Keywords: PEDOT, electrochromics, morphology, adhesion, electropolymerization

Poly(3,4-ethylenedioxythiophene) (**PEDOT**) is a well-known semiconducting polymer with favorable properties which find it often applied as the active material in biological sensors and electrochromic devices. However, **PEDOT** has several drawbacks which can prohibit its effective or long-term use, including weak adhesion to substrates such as ITO-coated glass, poorly controlled surface morphology, and reduced electrochemical stability over time. While a diverse range of approaches have been explored to overcome these issues, most involve additives or substrate modification, while solutions based on direct covalent adaptation are relatively lacking. We present a novel polymer based on covalently modified EDOT (**PEDOT-Crown**), featuring polar motifs and a 15-crown-5 moiety. Compared to **PEDOT**,

PEDOT-Crown demonstrates a wealth of advantageous properties including: superior adhesion to ITO under physical and electrochemical duress; a more uniform surface morphology; and electrochemical properties including a higher contrast ratio, red-shifted polaron and bipolaron absorption features, bleaching of the neutral absorption band across a narrower voltage range, and more Faradaic rather than capacitive behavior. Additionally, we note that in the presence of Na^+, **PEDOT-Crown** appears to show modified behavior in long-term electrochemical experiments. These features make **PEDOT-Crown** a material with improved suitability for application in biological sensing and electrochromic devices, compared to **PEDOT**.

1. Introduction

The structure-based tuneability of the electronic and optical properties of conjugated polymers have enabled their application across a range of fields, including optoelectronics,[1] energy harvesting,[2] electrochromics,[3,4] and biological sensing[5]. One of the most ubiquitous polymers across many of these fields today is poly(3,4-ethylenedioxythiophene) (**PEDOT**, **Figure 1**), whose enduring popularity stems from a plethora of advantageous features related to its molecular design. For example, the planar thiophene moiety enables the attainment of high hole mobility[6] while the ethylenedioxy bridge reduces the oxidation potential of thiophene, while simultaneously blocking the thiophene β-positions, thereby enabling **PEDOT** fabrication by electropolymerization, a property which eludes many other polythiophenes.[7,8] Electropolymerization is a desirable and convenient approach to polymer synthesis, because in addition to being a relatively straightforward method of producing polymers of high purity, it has the benefit of allowing polymerization directly onto an electrode or into a device channel, ready for use.[9] These characteristics, plus its flexibility and biocompatibility,[10] make **PEDOT** a widely used material for devices in biological sensing.[11] Furthermore, its well-established electrochromic switching between dark- and sky-blue has enabled the development of **PEDOT**-based electrochromic devices.[12]

Despite these advantages, there are still many obstacles yet to overcome in order to realize the full potential of **PEDOT** as an ideal bioelectronic or electrochromic material; noted problems associated with **PEDOT** include decay in stability over time;[12] poorly controlled surface morphology;[13] and weak substrate adhesion,[14] attributed to the lack of suitable chemical interactions between the substrate and polymer.[15] Much work has already been done to procure solutions to these issues; thus far mostly focusing on refining deposition method, or incorporating a variety of comonomers, dopants or additives.[16–19]

Another approach to improving the properties of **PEDOT** is by covalent modification;[20,21] as mentioned above, it is well known that small alterations to chemical structure can impact

greatly on many properties of conjugated polymers, from solution processability, to improved charge carrier mobility, to tailored optical properties. Examples of covalently modified **PEDOT**s are comparatively few compared to composites, due to known difficulties with the synthetic modification of EDOT. The issue is also complicated by the requirement for the monomer to retain its reactivity to electropolymerization, a feature which for example is lost through modification *via* "click" chemistry, due to the interference of the resulting triazole with radical cations.[22] Much endeavor has been undertaken to explore ways in which covalently modified EDOT species can be accessed, with highlights including the related 3,4-propylenedioxythiophene (ProDOT),[23,24] 3,4-phenylenedioxythiophene (PheDOT),[25] exomethylene-3,4-ethylenedioxythiophene (emEDOT),[26] or EDOT-carboxylic acids[27–29] and by use of the Staudinger-Vilarrasa reaction.[30]

Using methods such as these, access to **PEDOT**s with tailored pendant groups has been unlocked, and these materials have been successfully exploited to improve or introduce a diverse range of functionalities to the polymer. This includes improving substrate binding;[18,31] enhancing electrochromic properties with the inclusion of alkyl,[32] ethylene oxide,[33] or amino acid[34] motifs; and the introduction of selective analyte interaction to open the door to biological sensing, such as for chiral molecules,[35] metal ions[36–38] or oligonucleotides.[39]

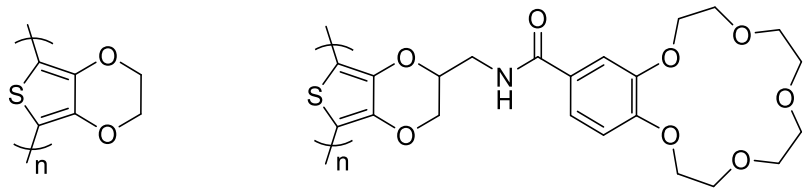

Figure 1. The structures of **PEDOT** and **PEDOT-Crown**

To that end, herein we present a novel, covalently modified **PEDOT-Crown** (**Figure 1**) which is shown to improve upon a variety of the aforementioned issues with **PEDOT** as a result of key features of its molecular design. After establishing the best conditions for electropolymerization using a **PEDOT** model, we compare the morphology, adhesion, and

electrochemical and optical properties, finding our new **PEDOT-Crown** to be superior across all aspects, in addition to observing potential ion-sensing functionality.

2. Results & discussion

2.1. Synthesis and electrochemical properties of a novel PEDOT-Crown polymer

2.1.1. Monomer design

For this work, we set out to design a novel EDOT-based monomer incorporating structural aspects which may contribute to the following criteria: encourage interaction with, and thus improve adhesion to, ITO-glass; increase rigidity in order to observe the effect on morphology; promote electrochemical and electrochromic activity in aqueous systems, and imbue potential sensing capability. Previously, oligoethers have been demonstrated to reduce film delamination while imparting good electrochemical properties in aqueous media, both of which are crucial properties for biological sensing, in addition to forming materials with high contrast ratios.[40,41] When translated to a crown ether, analyte specificity may also be introduced; incorporation of 15-crown-5, a well-known sodium-chelating group, can impart the capacity for a selective sensing response to Na^+, as previously recorded in analogous materials.[36,42,43] Synthetic route was also considered, and the Staudinger-Vilarrasa reaction[44] was selected as a suitable method, based on its prior success modifying EDOT to make electropolymerizable monomers in good yield[30] and the corresponding formation of an amide: a rigid and polar group which may aid adhesion to ITO, as has been demonstrated with other hydrogen-bonding carbonyl groups.[18]

2.1.2. Monomer synthesis

With this design in mind, a feasible pathway towards the monomer **EDOT-Crown** was conceived, adapted from previous works modifying EDOT[30] using the Staudinger-Vilarrasa reaction,[44] and based on the availability of the commercial starting reagents 3,4-dimethoxythiophene and 4'-carboxybenzo-15-crown-5 (depicted in **Scheme 1**). Intermediates **EDOT-Cl**[45] and **EDOT-N_3**[34] were synthesized in moderate to high yields according to the

literature, followed by the novel monomer **EDOT-Crown** in a yield of 72% with an overall 30% yield over 3 steps.

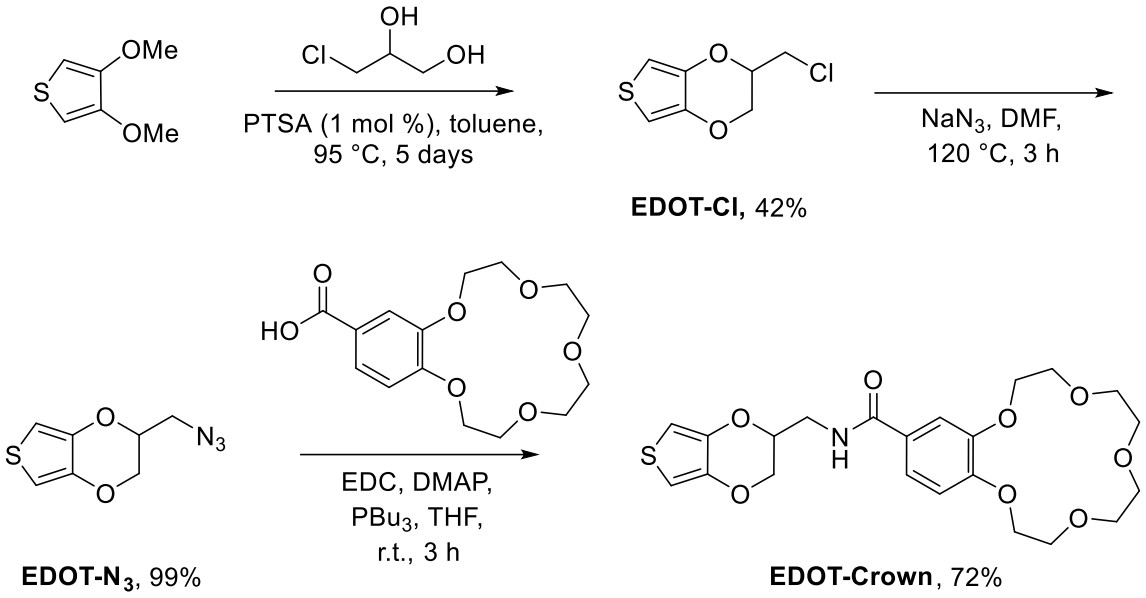

Scheme 1. Synthetic route towards the **EDOT-Crown** monomer.

2.1.3. Electrodeposition

Electropolymerized films of organic conjugated materials may be made either potentiodynamically (by cyclic voltammetry) or potentiostatically (by chronoamperometry). Altering various parameters within these methods can dramatically affect the thickness and morphology of the resulting polymer film. Prior to **EDOT-Crown** polymerization, the parameters of both electrochemical deposition methods were systematically investigated using **PEDOT** as a model, in order to establish the best conditions with which to make smooth, well-adhered polymer films of an optimal thickness for application as the active layer in transistors or in electrochromic devices, generally in the range of tens[46] to hundreds[47] of nm respectively. A full breakdown of the exploring of this parameter space is given in the Supporting Information. In summary, we found that the conditions which produce the best films for our purposes are: 10 mM monomer, with +1.2 V/45 sec for chronoamperometry or 10 scans -0.5 – +1.2 V at 0.1 V/s for cyclic voltammetry (for full synthetic procedures, refer to Section 4.2). Thus, all **PEDOT** and **PEDOT-Crown** films discussed henceforth use these

parameters for electropolymerization, with 0.1 M *N*-tetrabutylammonium perchlorate ($TBAClO_4$) in acetonitrile as the supporting electrolyte in order to avoid interaction between Na^+/15-crown-5 during film fabrication.

2.1.4. Electrochemical and spectroelectrochemical properties

After deposition, the fundamental electrochemical and spectroelectrochemical characteristics of the materials must be determined in order to identify the impact of these structural modifications and assess the applicability of these materials for use in in organic electronic devices. For example, electronic charge transport relies on oxidized or reduced (doped) species while electrochromic displays utilize spectral differences between neutral and charged species.

Films of **PEDOT-Crown** were analyzed by cyclic voltammetry and spectroelectrochemistry, and compared with **PEDOT** fabricated in the same conditions. Detailed below, we find that despite their shared EDOT backbone motif, the **PEDOT** and modified **PEDOT-Crown** polymers exhibit great disparity in their (spectro)electrochemical characteristics.

Cyclic voltammetry

Inspection of cyclic voltammograms in **Figure 2** reveals a near-capacitive process for **PEDOT** compared to a more Faradaic behavior for **PEDOT-Crown** in both aqueous and organic systems. Clear reversible redox is observed to occur for the **PEDOT-Crown**; with the onset of the major oxidation event around -0.27 V in acetonitrile and -0.12 V in H_2O *vs*. Ag/Ag^+, and half-wave potentials calculated to be -0.09 V and +0.32 V respectively. We speculate that the different electrochemical behavior of the two systems is related to different solid-state morphologies and different degrees of polymer backbone planarity (*vide infra*). It should be noted that the capacitive and Faradaic behavior of conducting polymers is still the subject of debate and ongoing investigations.[48–50]

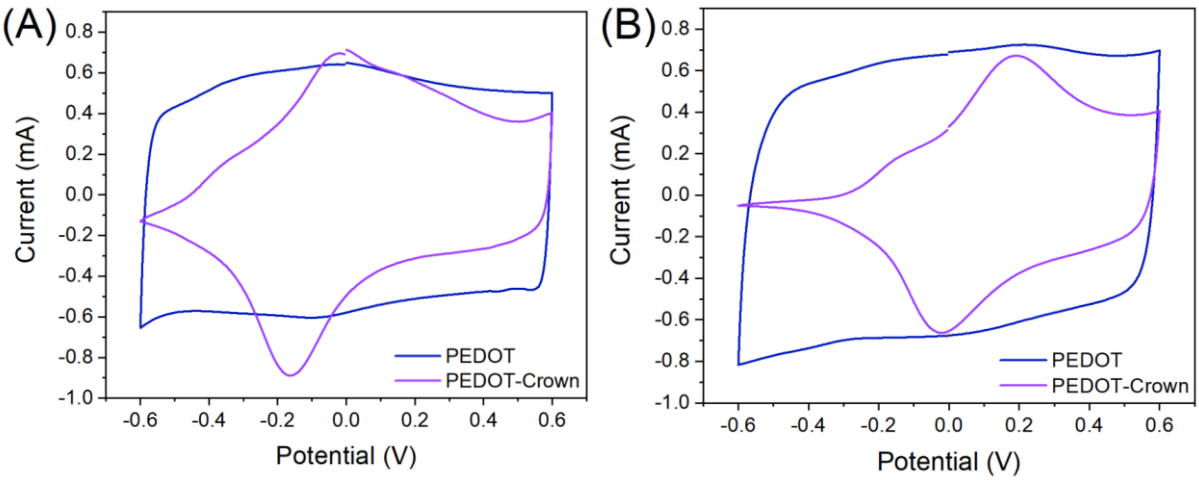

Figure 2. Overlaid 3rd scan of cyclic voltammograms (range -0.6 V to +0.6 V, scan rate 0.05 V/s) of **PEDOT** (blue) and **PEDOT-Crown** (purple) thin films deposited on ITO-glass by chronoamperometry (+1.2 V, 45 sec, 10 mM EDOT) in a) 0.1 M $TBAClO_4$ in acetonitrile; b) 0.1 M $NaClO_4$ in H_2O.

Spectroelectrochemistry

Spectroelectrochemical analysis of thin films of **PEDOT** and **PEDOT-Crown** polymerized by chronoamperometry (+1.2 V, 45 sec, 10 mM EDOT) was conducted by stepwise electrochemical oxidation with concurrent recording of the UV-Vis-NIR absorption spectrum at each potential. While the degree of bleaching of the neutral absorption features upon oxidation provides information about whether the entire film can be oxidized, the emerging spectral features provide information about the structure and stability of the oxidized species. These spectroelectrochemical studies reveal several differences between the two systems. Aqueous electrolyte conditions (0.1 M $NaClO_4$ in H_2O) were used to assess the applicability of these materials for use in bioelectronics. The results, given in **Figure 3**, show **PEDOT-Crown** to display several features which distinguish it favorably from **PEDOT**.[51] First, both the polaron and bipolaron absorption maxima (λ_{max}) of **PEDOT-Crown** are substantially red-shifted in comparison to **PEDOT,** at values of 986 nm and 865 nm respectively for the polaron, (**Table 1**) and 1324 nm for the **PEDOT** bipolaron, compared to a wavelength which exceeded the range of this study for **PEDOT-Crown** (>1350 nm). We ascribe these red-

shifted features for **PEDOT-Crown** to a longer effective conjugation length resulting in more delocalized polaronic and bipolaronic states compared to **PEDOT**. Besides the obvious impact on color changes upon electrochemical switching, this could also lead to more mobile charge carriers, thus impacting both electrochromic and transistor-based devices.

Table 1. λ_{max} values for the neutral, polaron and bipolaron peaks of **PEDOT** and **PEDOT-Crown**.

Material	$\lambda_{neutral}$	$\lambda_{polaron}$	$\lambda_{bipolaron}$
PEDOT	570	865	1324
PEDOT-Crown	596	986	>1350[a)]

Values taken from spectra of absorbance difference to -0.6 V. [a)]Absorption maxima for **PEDOT-Crown** bipolaron exceeds the measured range (>1350 nm); above which H_2O prohibits UV-Vis measurement of the thin film due to a dominant O-H stretching overtone.

Second, the **PEDOT-Crown** exhibits oxidation in two distinct phases; the polaron is formed between -0.3 to 0.0 V simultaneously with the quenching of the π-π* band, while above this range the polaron is depleted while the bipolaron emerges (**Figure S3**). In contrast, the **PEDOT** thin film demonstrates no discrete polaron formation, with the dication emerging almost concurrently. Third, for **PEDOT-Crown,** bleaching of the neutral absorption band occurs mostly within the narrow range of -0.1 V to +0.2 V (a window of around 0.3 V), whereas the equivalent process for **PEDOT** is much more gradual, occurring over a wide range between -0.6 and +0.1 V (window 0.7 V), shown in **Figure S4.** Efficient bleaching of the neutral absorption band, as seen for both polymers, indicates suitability for electrochemical operation in aqueous media, as required for many bioelectronic applications. Being able to generate either the polaron or bipolaron more selectively, as observed for **PEDOT-Crown**, indicates better control of the absorption in the near-infrared region. In addition, in some cases, polarons are noted to be more mobile than bipolarons, so this could also be harnessed advantageously in transistor-based devices.[52–54] These observations are supported by the differences seen for the neutral states; alongside the neutral λ_{max} at 596 nm, we note the presence of a shoulder at approximately 650 nm for the **PEDOT-Crown**, which,

in the solid state, is assigned by Spano to be the 0-0 vibronic transition in a H- or J-like aggregated system, representative of a highly ordered system;[55,56] no such feature is observed for **PEDOT**.

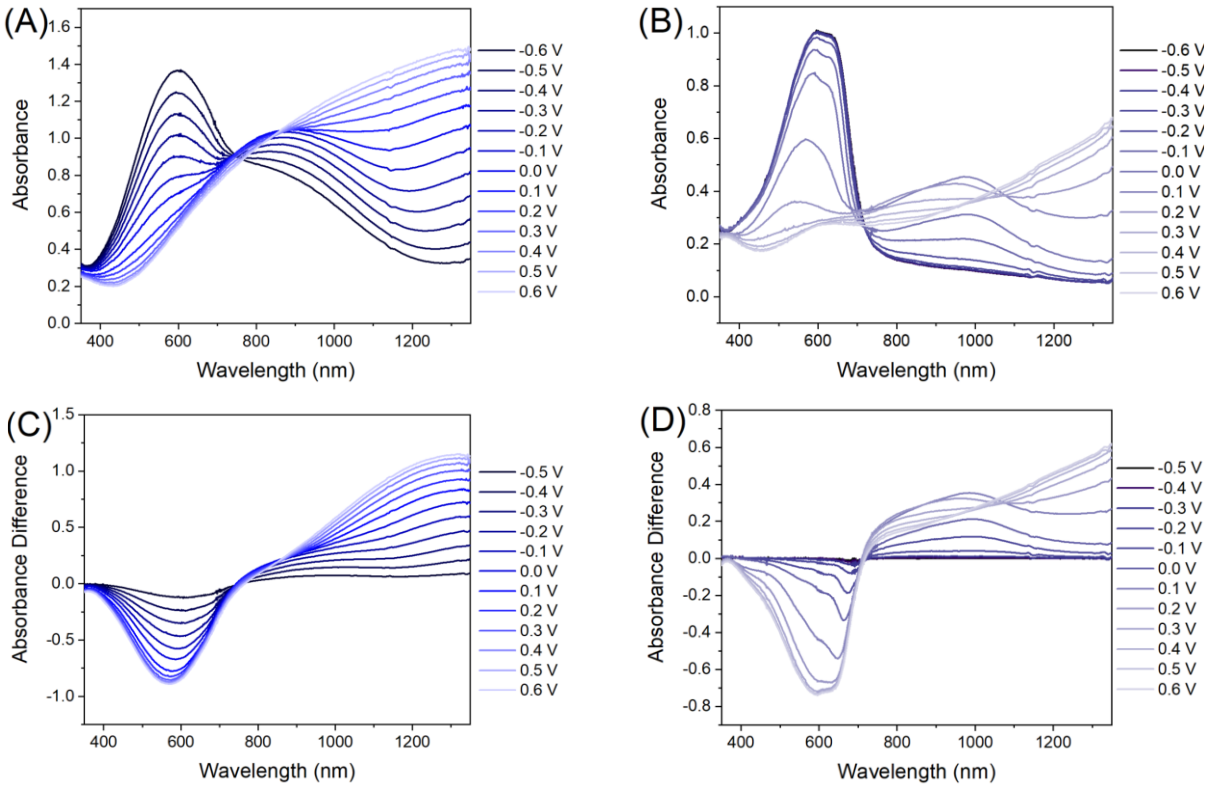

Figure 3. Spectroelectrochemical analysis of polymer thin films deposited on ITO-glass by chronoamperometry (+1.2 V, 45 sec, 10 mM monomer) a) **PEDOT** and b) **PEDOT-Crown** in 0.1 M $NaClO_4$ in H_2O; plotted as difference *vs*. neutral polymer (at -0.6 V) for c) **PEDOT** and d) **PEDOT-Crown**.

2.2. Comparing adhesion, physical integrity and morphology for device applicability

In addition to electrochemical properties, physical durability, strength of substrate adhesion and film morphology are critically important to the functionality and applicability of these materials. In this section, we show that **PEDOT-Crown** displays enhanced adhesion to ITO-glass, under both physical and electrochemical duress, in addition to a smoother surface profile and a more compact morphology.

2.2.1. Adhesion, integrity and cycling stability

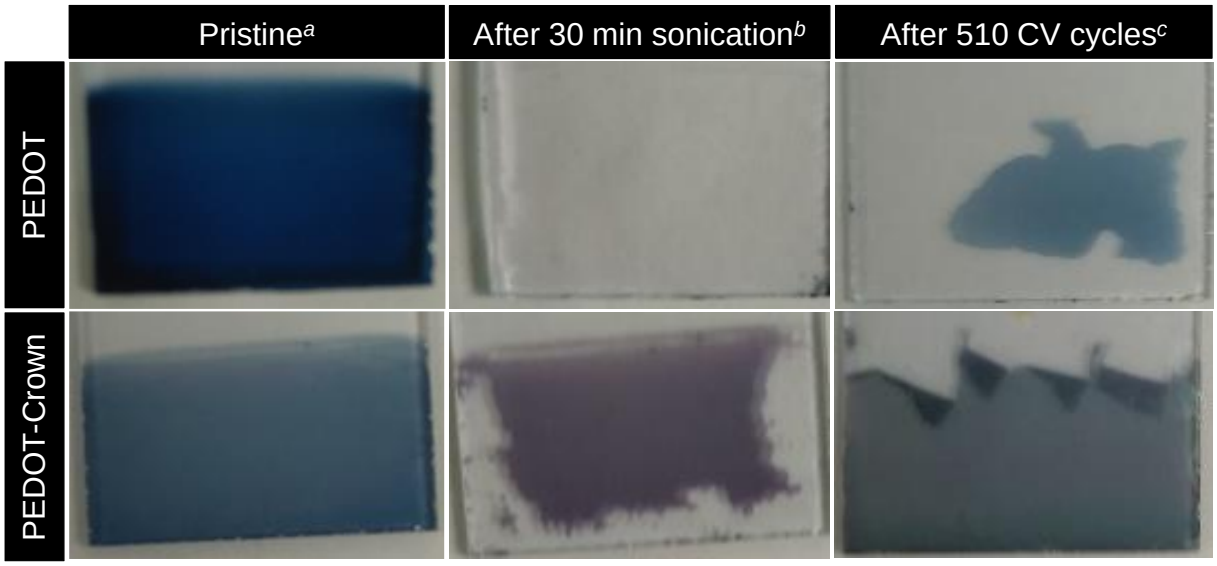

Figure 4. Photographs of **PEDOT** and **PEDOT-Crown** films on ITO-coated glass a) immediately after deposition by chronoamperometry (+1.2 V, 45 sec, 0.1 M $TBAClO_4$ in acetonitrile); b) after ultrasonication in H_2O (r.t., 30 min); c) after 510 CV cycles (-0.6 – +1.2 V, 0.3 V/s) in 1X PBS solution (pH 7.4).

While previous works have enhanced the adhesion of **PEDOT** to tin-oxide based substrates via pre-polymerization surface modification with intermediary polar EDOT groups,[18,57–59] here we demonstrate that a comparable improvement can be achieved without the use of a separate species as an additive layer, by incorporating polar moieties directly into the polymer structure which may encourage binding interaction with the polar groups on the ITO surface. With pristine films pictured in **Figure 4a** for reference, in **Figure 4b**, it can be seen that a film

of **PEDOT-Crown** remains largely intact on the surface of an ITO-coated glass substrate after 30 mins sonication in H_2O, while a **PEDOT** film prepared under identical conditions is completely delaminated. In addition to this improved resistance to physical duress, the **PEDOT-Crown** polymer is also more able to withstand prolonged application of sweeping electrical voltage. In **Figure 4c**, the **PEDOT-Crown** film remains largely adhered to the ITO surface with only a minimal amount of peeling after application of 510 CV cycles (-0.6 – +1.2 V) in phosphate-buffered saline solution (1X PBS, pH 7.4), while the equivalent **PEDOT** film shows a greater extent of delamination in the same conditions, indicating that it may be less suitable for electrochemical applications in biological media. Cycling stability data for the first 205 cycles of this experiment is given in **Figure S5.**

2.2.2. Surface profile

Surface profile measurements of **PEDOT** and **PEDOT-Crown** films on ITO-coated glass illustrate clear differences in film thickness and morphology. When deposited by chronoamperometry (**Table 2**, **Figure S6a** and **S6c**), both polymers have an average thickness close to 0.5 µm, which is within the range of applicability for transistor and electrochromic devices.[46,47] However, when roughness is considered, the **PEDOT-Crown** film (**Figure S6c**) exhibits a far smoother and more uniform profile than its **PEDOT** counterpart (**Figure S6a**) also denoted numerically by the standard deviation, given in **Table 2.** Likewise, the **PEDOT-Crown** film produced by cyclic voltammetry (**Figure S6d**) is smoother than the corresponding **PEDOT** film (**Figure S6b**), but in this case, it is worth noting that the increased average **PEDOT** film thickness is skewed by the high degree of noise, which is attributed to puckering of the poorly-adhered thick film to ITO, as seen in **Figure S2**.[13,19] Therefore, this observed reduction in wrinkling for the **PEDOT-Crown** films is further evidence that the crown polymer achieves superior adhesion to ITO than is the case for **PEDOT**.

Table 2. Average thickness and roughness of films.

Material	Chronoamperometry (+1.2 V, 45 sec)		Cyclic voltammetry (-0.5 – +1.2 V, 10 scans)	
	Avg. thickness x̄ (μm)[a]	Roughness (σ)[b]	Avg. thickness x̄ (μm)[a]	Roughness (σ)[b]
PEDOT	0.54	0.21	2.36	1.14
PEDOT-Crown	0.47	0.047	1.26	0.20

As calculated from surface profile; data is the average of three measurements for each film

[a)]mean height profile 0-3 mm lateral; [b)]standard deviation 0-3 mm lateral.

2.2.3. Surface morphology

Morphology differences are also observed between the two polymer films at a microscopic level. Scanning electron microscopy (SEM) and atomic force microscopy (AFM) images were captured of films deposited by chronoamperometry. The SEM images in **Figure 5** reveal that the **PEDOT-Crown** polymer has a much smoother and more compact surface morphology than **PEDOT**. Further examination by AFM confirms this structure, in addition to providing the roughness measurements in **Table 3**, wherein the roughness of **PEDOT** is approximately 4× that of **PEDOT-Crown**, in line with surface profile measurements. In **Figure 5,** it is important to note the difference in scale used to illustrate depth for polymers in AFM: due to the substantially different thickness and uniformity between the two polymer films, a consistent scale could not be used to represent the morphology of both surfaces in good detail, and thus **PEDOT** is scaled to a wider range accordingly (-500 to 700 nm) than the much thinner and more uniform **PEDOT-Crown** (-150 nm to 250 nm). AFM images alongside rescaled counterparts for comparison are available in **Figure S7.**

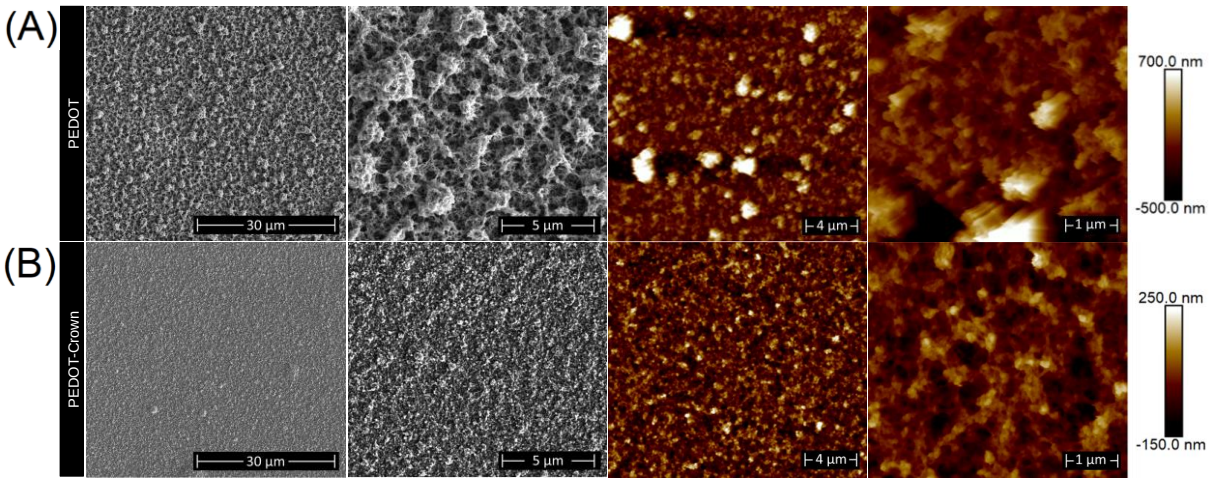

Figure 5. Topographical images of polymers a) **PEDOT** and b) **PEDOT-Crown** deposited by chronoamperometry (+1.2 V, 45 sec, 0.1 M $TBAClO_4$ in acetonitrile); SEM on Cr/Au (10 nm/100 nm) coated polyimide substrates (left) and AFM on ITO-coated glass (right).

Table 3. Roughness measurements of **PEDOT** and **PEDOT-Crown**.

AFM image	R_a (nm)[a]	R_q (nm)[b]
PEDOT: 5 µm scale	171	254
PEDOT: 20 µm scale	142	205
PEDOT-Crown: 5 µm scale	42.0	52.5
PEDOT-Crown: 20 µm scale	45.7	58.1

As calculated from AFM (tapping mode): [a)]average surface roughness for whole image; [b)]root mean square roughness for whole image.

2.3. Electrochromic switching and sodium response

2.3.1. Contrast ratio

Based on the spectroelectrochemistry data in **Figure 3,** from which the absorption minima and maxima for the neutral **PEDOT-Crown** polymer were obtained at +0.5 V and -0.3 V respectively, these voltages were applied as the oxidative and reductive potentials in electrochromic switching experiments for both materials. Voltages were applied sequentially

for 30 seconds each, over 200 cycles, in either organic (acetonitrile, 0.1 M $TBAClO_4$) or aqueous (H_2O, 0.1 M $NaClO_4$) systems and the change in transmittance (ΔT%) was recorded. Initial switching ΔT% values are extracted from the 11th switching cycle, allowing for redox equilibration in the film over the first 10 cycles.[60] These are compared with values from the final, 200th cycle in the experiment, to observe any differences in ΔT% and switching time during the process. The results, presented in **Table 4** and **Figure 6**, demonstrate that the **PEDOT-Crown** film achieves both a higher transparency when oxidized (T_{ox}%) and a superior overall contrast ratio (ΔT%) than the equivalent **PEDOT** film under the same conditions; values of 45-50% T_{ox} and 35-46% ΔT compared to 23-26% T_{ox} and 11-12% ΔT were observed for **PEDOT-Crown** and **PEDOT**, respectively. Based on the **PEDOT** spectroelectrochemistry, a wider voltage range of -0.6 and +0.5 V was then applied to investigate whether this would facilitate a comparable T_{ox}% and ΔT% for the **PEDOT** film; however, even with the greater reducing potential applied, T_{ox} above 32% and ΔT above 20% were not achieved. Additionally, the contrast ratio decayed by more than half of its initial value (from 20% to 9%) upon repeated cycling in the organic system at this wider voltage range, while in the aqueous system, a partial delamination of the **PEDOT** film occurred (**Figure S8**).

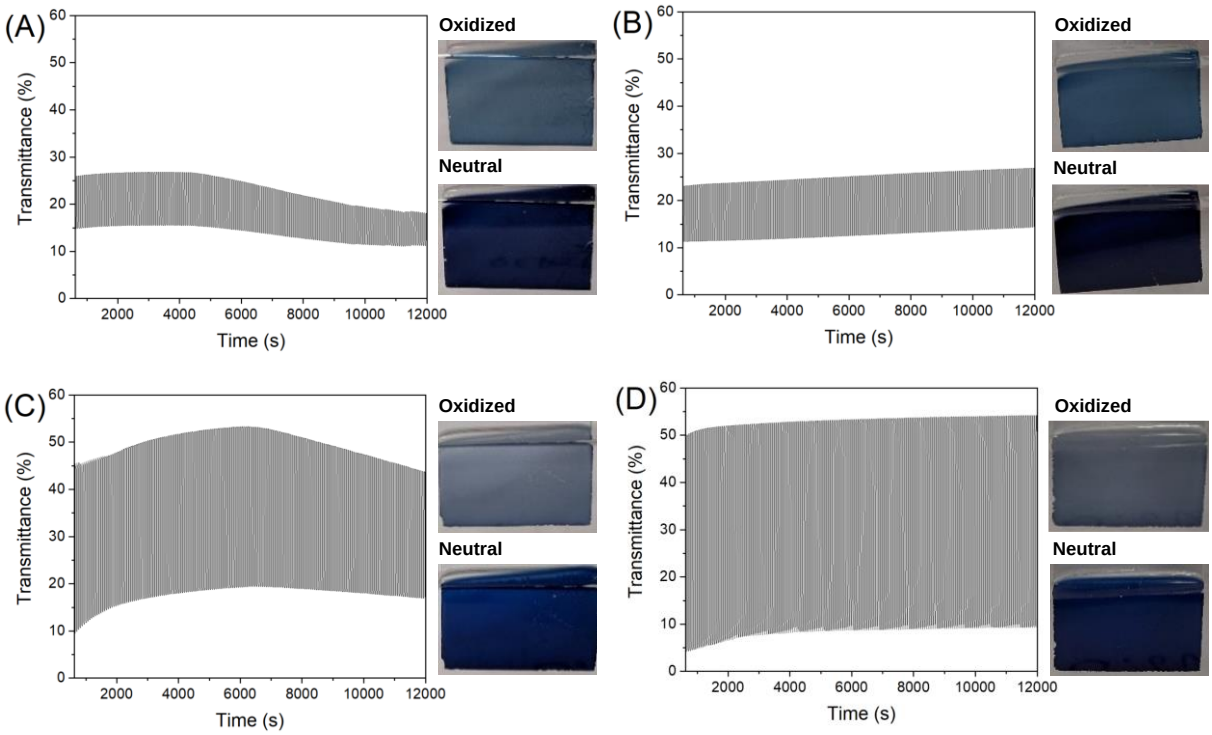

Figure 6. Electrochromic switching between -0.3 V and +0.5 V for 30 second cycles (cycles 11-200 shown) with corresponding oxidized/neutral film colors for a) **PEDOT** with 0.1 M $TBAClO_4$ in MeCN b) **PEDOT** with 0.1 M $NaClO_4$ in H_2O c) **PEDOT-Crown** with 0.1 M $TBAClO_4$ in MeCN d) **PEDOT-Crown** with 0.1 M $NaClO_4$ in H_2O. Films deposited onto ITO-glass substrates by chronoamperometry (+1.2 V, 45 sec, 10 mM monomer).

Table 4. Electrochromic switching behavior of **PEDOT** and **PEDOT-Crown**.

Film	Solvent, Electrolyte	Wavelength (nm)	Voltage	$T\%_{ox}$ [a]	$T\%_{red}$ [b]	$\Delta T\%_{init.}$ [c]	$\Delta T\%_{200}$ [d]
PEDOT-Crown	MeCN, 0.1 M $TBAClO_4$	575	-0.3 V, +0.5 V	44.5	9.5	35.0	26.7
PEDOT-Crown	H_2O, 0.1 M $NaClO_4$	575	-0.3 V, +0.5 V	50.0	4.4	45.6	43.8
PEDOT	MeCN, 0.1 M $TBAClO_4$	600	-0.3 V, +0.5 V	25.9	14.8	11.1	6.8
PEDOT	H_2O, 0.1 M $NaClO_4$	600	-0.3 V, +0.5 V	23.0	11.3	11.7	12.6

PEDOT	MeCN, 0.1 M $TBAClO_4$	600	-0.6 V, +0.5 V	31.6	11.9	19.7	9.3
PEDOT	H_2O, 0.1 M $NaClO_4$	600	-0.6 V, +0.5 V	19.0	1.6	17.4	18.1

[a)]Midpoint T% for oxidized polymer, 11th cycle [b)]Midpoint T% for reduced polymer, 11th cycle [c)] Midpoint T_{ox}-T_{red} for 11th cycle [d)] Midpoint T_{ox}-T_{red} for 200th cycle

2.3.2. Behavior in the presence of sodium

The electrochromic switching experiment also revealed interesting preliminary behavior unique to the **PEDOT-Crown** film in the presence of Na^+. Closer inspection of the first and last 10 cycles of the experiment reveals that both materials initially exhibit a comparably fast switching capacity ($\Delta T\%_{init}$ reaches >99% of its total switch within 3 sec) giving rise to the rectangular shape of the T% response to potential in **Figure 7**. However, it is worth noting that within this time, the **PEDOT-Crown** completes a ΔT% of more than 3× the magnitude of **PEDOT** in both systems, despite its more compact morphology (**Figure 5**). We note that **PEDOT-Crown** in an aqueous environment, which is the only system to contain 15-crown-5 with its corresponding chelating ion Na^+, is the only film in the series in which a notable decay in switching rate over time is observed. In cycles 191-200 (**Figure 7d**), a curved ΔT% response *vs.* time is observed, reaching only 63% of the total $\Delta T\%_{200}$ within 3 sec and 92% within 6 sec, compared to ≥95% within 3 sec for the other three systems (**Figure 7a-c**, **Table 5**). While this long-term change in temporal response cannot be attributed with certainty to crown/Na^+ interaction at this stage, it is worth noting that it corroborates observed results from Salinas *et al.* with a similar crown ether functionalized **PEDOT** film, in which a 25% decay of maximum conductance over 50 cycles was observed compared to <10% for **PEDOT** and ion controls.[36]

Table 5. Electrochromic switching response times of **PEDOT** and **PEDOT-Crown**.

Film	Solvent, Electrolyte	Wavelength (nm)	Voltage	% total ΔT reached within 3 sec of potential switch (init.)[a]	% total ΔT reached within 3 sec of potential switch (cycle 200)[b]
PEDOT-Crown	MeCN, 0.1 M $TBAClO_4$	575	-0.3 V, +0.5 V	100	>99
PEDOT-Crown	H_2O, 0.1 M $NaClO_4$	575	-0.3 V, +0.5 V	>99	63
PEDOT	MeCN, 0.1 M $TBAClO_4$	600	-0.3 V, +0.5 V	99	95
PEDOT	H_2O, 0.1 M $NaClO_4$	600	-0.3 V, +0.5 V	99	99

[a])$(T\%_{3sec}-T\%_{red})/\Delta T\%$ 11th cycle, [b])$(T\%_{3sec}-T\%_{red})/\Delta T\%$ 200th cycle

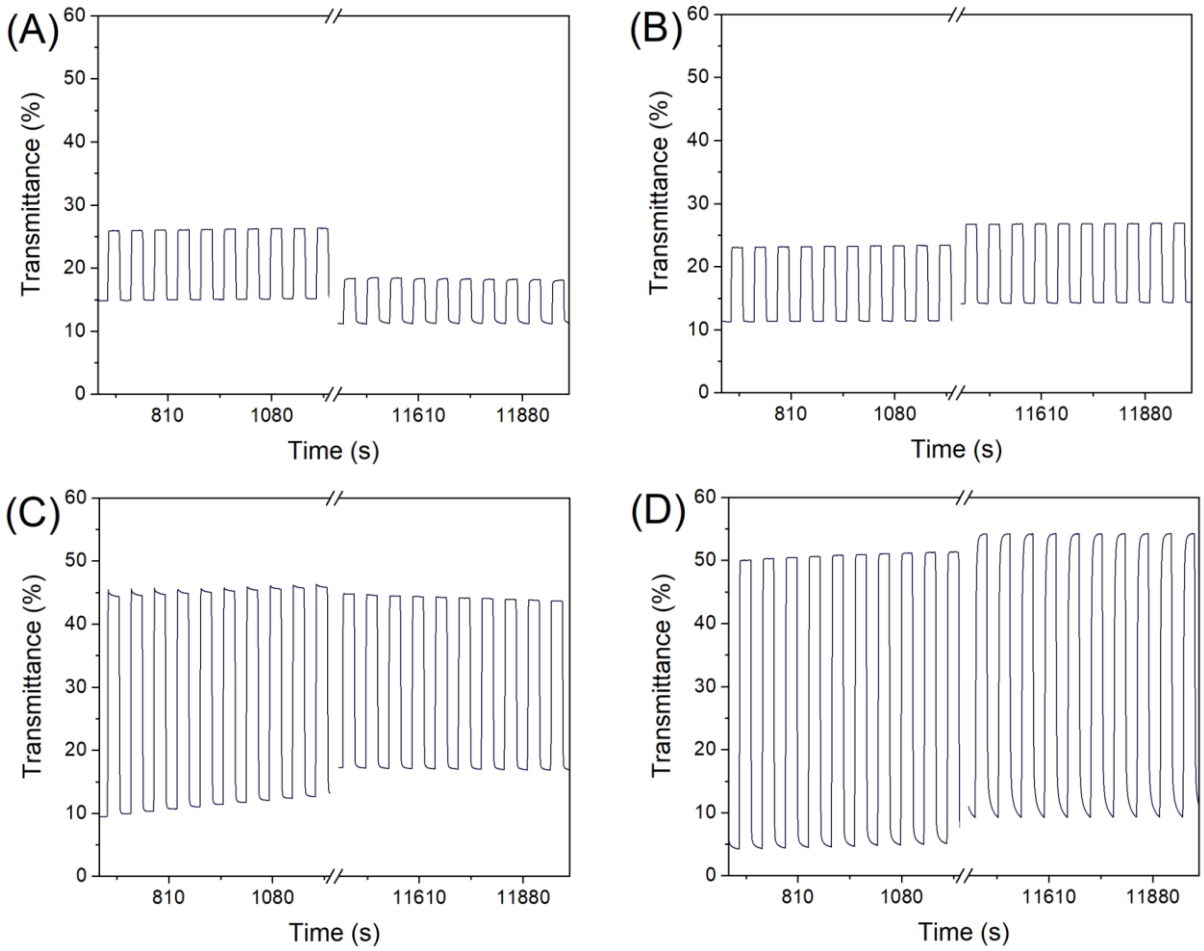

Figure 7. Close up of electrochromic switching cycles 11-20 (initial) vs.191-200 (last) between -0.3 V – +0.5 V for a) **PEDOT** with 0.1 M $TBAClO_4$ in MeCN b) **PEDOT** with 0.1 M $NaClO_4$ in H_2O c) **PEDOT-Crown** with 0.1 M $TBAClO_4$ in MeCN d) **PEDOT-Crown** with 0.1 M $NaClO_4$ in H_2O

3. Conclusion

After extensive investigation into the optimal conditions with which to deposit **PEDOT** films by both cyclic voltammetry and chronoamperometry, we found the best parameters for deposition to be 10 scans from -0.5 to +1.2 V at 0.1 V/s, and +1.2 V for 45 sec, respectively, with 10 mM monomer concentration in acetonitrile. These methods were then applied to make thin-films of **PEDOT** alongside a new, covalently-modified EDOT-based material, **PEDOT-Crown**, and the two were compared for their physical and electrochemical properties. We find that **PEDOT-Crown** exhibits many characteristics which make it superior to **PEDOT** for applications in electrochromic devices and biological sensing. These include: morphology and integrity characteristics, such as improved adhesion to ITO-glass substrates, with smoother surface morphology and the increased ability to tolerate physical and electrochemical duress; spectroelectrochemical properties, such as red-shifted polaron and bipolaron λ_{max} values and neutral absorption band bleaching within a narrower voltage range; and electrochromic properties, such as higher transparency and contrast ratio. Finally, we note a preliminary finding that **PEDOT-Crown** may exhibit a modified response in long-term electrochromic switching experiments, in the presence of the chelating Na^+ ion, which was not observed in the **PEDOT** or TBA^+ controls, opening the door to future work exploring its use as an ion sensor.

4. Experimental

4.1. Materials and measurements

Reactions were carried out using commercially available reagents, used as supplied as follows: EDOT, 3,4-dimethoxythiophene, *p*-toluenesulfonic acid monohydrate, NaN_3, DMAP, *N*-(3-dimethylaminopropyl)-*N*'-ethylcarbodiimide, and $TBAClO_4$ from Fluorochem; tributylphosphine and 4'-carboxybenzo-15-crown-5 from Sigma Aldrich; $NaClO_4$ and (±)-3-chloro-1,2-propanediol from Alfa Aesar, in combination with solvents from Honeywell and anhydrous solvents from Acros Organics. Column chromatography was carried out using VWR silica gel (40-60 μm). Analytical thin layer chromatography was carried out on Merck Kieselgel 60 aluminium-backed silica plates, with visualization using short-wave ultraviolet light. Electrochemistry experiments were carried out using a PalmSens EmStat3+ potentiostat. Working electrodes were either ITO-coated glass (20 mm × 20 mm) for films made for CV, UV-Vis, surface profile measurements and AFM, or Cr/Au (10 nm/100 nm) coated Kapton 500HN polyimide sheet (7 mm × 30 mm) for SEM. Counter electrodes were Pt wire, or alternatively Pt mesh (20 mm × 20 mm) for experiments with ITO-glass. Reference electrodes were $Ag/AgNO_3$ in MeCN for organic systems or Ag/AgCl in H_2O for aqueous systems. ITO slides were plasma cleaned in a Harrick PDC-32G-2 plasma cleaner. UV-Vis measurements were obtained from a Shimadzu UV-3600 Plus UV-Vis-NIR spectrophotometer. ^{1}H NMR spectra were recorded at 400 MHz on a Bruker Avance III spectrometer. Chemical shifts (δ) are quoted to the nearest 0.01 ppm relative to tetramethylsilane, with the residual solvent peak $CHCl_3$ used as the internal standard (7.26 ppm). Coupling constants (*J*) are given to the nearest 0.1 Hz. Peak multiplicities for resonances are noted as: s, singlet; d, doublet; dd, doublet of doublets; t, triplet; m, unresolved multiplet. ^{13}C NMR spectra were recorded at 101 MHz on a Bruker Avance III spectrometer. Chemical shifts (δ) are quoted to the nearest 0.1 ppm, with reference to the given solvent $CDCl_3$ (77.0 ppm) as the internal standard. ^{1}H and ^{13}C NMR spectra are provided in the Supporting Information. Low-resolution mass spectra were obtained from an Agilent 6890N Gas Chromatograph, and high-resolution mass spectra were obtained from a Waters Synapt G2-Si High-Definition Mass Spectrometer. Melting

points were obtained using a Stuart SMP11 melting point apparatus and are uncorrected. Surface profile measurements were taken using a Bruker DektakXT Stylus Profiler. SEM images were captured using an FEI Quanta 3D electron microscope, with the operating parameters as follows; accelerating voltage 2 kV, probe current 33 pA, working distance 5 mm. AFM images were captured in tapping mode using a Bruker Dimension Icon scanning probe microscope with a Bruker ScanAsyst-Air silicon tip on nitride lever.

4.2. Synthesis of EDOT-Crown

Synthetic procedures towards **EDOT-Crown** were carried out in a sealed environment under a nitrogen atmosphere, using glassware oven-dried at 120 °C overnight. "H_2O" refers to deionized water throughout. Intermediates **EDOT-Cl**[45] and **EDOT-N_3**[34] were synthesized according to the literature, while **EDOT-Crown** was synthesized adapted from previous covalent modifications of EDOT[30] using the Staudinger-Vilarrasa approach.[44]

4.2.1. General procedure for electropolymerizations

For polymerizations onto ITO-glass, slides were cleaned with detergent followed by sonication in H_2O (3 × 15 min), acetone (2 × 10 min), and isopropyl alcohol (2 × 5 min), followed by plasma cleaning for 5 min directly before use. Gold electrodes were cleaned by cyclic voltammetry in 10 mM H_2SO_4 aq. (10 cycles -0.2 – +1.4 V), rinsed with H_2O and dried under a jet of N_2. Unless otherwise stated, electropolymerizations were carried out in ambient conditions from 10 mM monomer solutions in degassed MeCN, with 0.1 M $TBAClO_4$ as supporting electrolyte; using +1.2 V/45 sec for chronoamperometry or 10 scans -0.5 – +1.2 V at 0.1 V/s for cyclic voltammetry.

*4.2.2. 2-(Chloromethyl)-2,3-dihydrothieno[3,4-b][1,4]dioxine (**EDOT-Cl**)*

Under an atmosphere of nitrogen, 3,4-dimethoxythiophene (5.0 g, 35 mmol, 1.0 eq.), 3-chloro-1,2-propanediol (7.25 mL, 88 mmol, 2.5 eq.) and *p*-toluenesulfonic acid monohydrate (66 mg, 0.35 mmol, 1 mol%) were dissolved in anhydrous toluene (140 mL) in a 250 mL 2-necked

round bottom flask equipped with distillation apparatus. The solution was heated at 95 °C for 24 h, over which time a black oily suspension was formed. After this time, another equal portion of the diol (7.25 mL, 88 mmol, 2.5 eq.) was added and the mixture was stirred at the same heat for a further 4 days, then cooled to room temperature. The toluene solution was decanted from the insoluble oil and concentrated *in vacuo.* The crude material was purified by chromatography over silica gel, with the **EDOT-Cl** eluting in 7:3 hexane:DCM as a white solid (2.76 g, 42%), R_f = 0.25. mp 41-43 °C; ^{1}H NMR (400 MHz, $CDCl_3$, δ): 6.36 (s, 2H), 4.40-4.34 (m, 1H), 4.28 (dd, *J* = 11.7 Hz, *J* = 2.2 Hz, 1H), 4.15 (dd, 1H, *J* = 11.7 Hz, *J* = 6.2 Hz), 3.75-3.64 (m, 2H); ^{13}C NMR (101 MHz, $CDCl_3$, δ): 141.3, 140.8, 100.3 (× 2), 73.0, 65.7, 41.5; GCMS (EI): *m/z* [M^+] calcd for $C_7H_7O_2ClS$ 190.0; found, 190.0, in accordance with literature.[45]

*4.2.3. 2-(Azidomethyl)-2,3-dihydrothieno[3,4-b][1,4]dioxine (**EDOT-N$_3$**)*

Under anhydrous conditions, **EDOT-Cl** (100 mg, 0.52 mmol, 1.0 eq.) was dissolved in anhydrous DMF (5.3 mL). To this solution, NaN_3 (44 mg, 0.68 mmol, 1.3 eq.) was added and the solution was heated to 120 °C and stirred at this temperature for 24 h. After this time, the solution was cooled to room temperature and H_2O (5.0 mL) was added. The mixture was extracted with EtOAc (50 mL) and washed with H_2O (1 × 50 mL) and brine (3 × 50 mL). Combined organic fractions were dried over $MgSO_4$, filtered and concentrated *in vacuo*. The crude material was purified by column chromatography over silica gel, with the **EDOT-N$_3$** eluting in 10% EtOAc in hexane as a pale yellow oil (101 mg, 99%) R_f = 0.29. ^{1}H NMR (400 MHz, $CDCl_3$, δ): 6.37 (dd, 2H, *J* = 16.0 Hz, *J* = 3.7 Hz), 4.34-4.29 (m, 1H), 4.20 (dd, 1H, *J* = 11.7 Hz, *J* = 2.3 Hz), 4.05 (dd, 1H, *J* = 11.7 Hz, *J* = 6.8 Hz), 3.60-3.47 (m, 2H); ^{13}C NMR (101 MHz, $CDCl_3$, δ): 141.2, 140.8, 100.4, 100.2, 72.5, 65.9, 50.6; GCMS (EI): *m/z*: [M^+] calcd for $C_7H_7N_3O_2S$ 197.0; found, 197.0, in accordance with literature.[34,61]

*4.2.4. N-((2,3-Dihydrothieno[3,4-b][1,4]dioxin-2-yl)methyl)-2,3,5,6,8,9,11,12-octahydrobenzo[b][1,4,7,10,13]pentaoxacyclopentadecine-15-carboxamide (**EDOT-Crown**)*

Under anhydrous conditions, 4-carboxybenzo-15-crown-5 (594 mg, 1.90 mmol, 1.5 eq.) was dissolved in anhydrous THF (25 mL) and DMAP (341 mg, 2.79 mmol, 2.2 eq.) was added. The mixture was cooled to 0 °C, and *N*-(3-dimethylaminopropyl)-*N*'-ethylcarbodiimide (354 mg, 2.28 mmol, 1.8 eq.) was added. The reaction was warmed to ambient temperature and stirred for 30 min. After this time, **EDOT-N$_3$** (250 mg, 1.27 mmol, 1.0 eq.), dissolved separately in anhydrous THF (5 mL), was added. The mixture was cooled to 0 °C, and tributylphosphine (0.63 mL, 2.53 mmol, 2.0 eq.) was added dropwise. The reaction was warmed to ambient temperature and stirred for a further 3 h, then concentrated *in vacuo* and purified by column chromatography over silica gel. The product eluted in 5:5:90 Et_3N:MeOH:EtOAc (R_f = 0.47) as a white powder, which was dissolved in the minimum amount of hot $CHCl_3$ and added to ice-cold Et_2O (50 mL). The resulting precipitate was collected and dried by vacuum filtration, to afford pure **EDOT-Crown** as a white solid (424 mg, 72%). mp 144-146 °C; ^{1}H NMR (400 MHz, $CDCl_3$, δ): 7.39 (d, 1H, *J* = 2.1 Hz), 7.28 (dd, 1H, *J* = 8.3 Hz, *J* = 2.1 Hz), 6.85 (d, 1H, *J* = 8.3 Hz), 6.45 (t, 1H, *J* = 5.8 Hz), 6.36-6.34 (m, 2H), 4.40-4.35 (m, 1H), 4.27 (dd, 1H, *J* = 11.8 Hz, *J* = 2.2 Hz), 4.20-4.16 (m, 4H), 3.99 (dd, 1H, *J* = 11.8 Hz, *J* = 7.7 Hz), 3.94-3.90 (m, 4H), 3.87-3.81 (m, 1H), 3.78-3.74 (m, 8H), 3.72-3.65 (m, 1H); ^{13}C NMR (101 MHz, $CDCl_3$, δ): 167.5, 152.4, 149.1, 141.6, 141.4, 126.9, 120.2, 113.3, 112.6, 100.1, 100.0, 73.0, 71.3, 70.6, 70.5, 69.5, 69.4, 69.2, 68.9, 66.5, 40.2. HRMS (ESI) *m/z* $[M + H]^+$ calcd for $C_{22}H_{28}NO_8S$ 466.1530; found, 466.1717.

Supporting Information

Supporting Information is available from the Wiley Online Library or from the author.

Received: ((will be filled in by the editorial staff))

Revised: ((will be filled in by the editorial staff))

Published online: ((will be filled in by the editorial staff))

References

1. Murad, A. R., Iraqi, A., Aziz, S. B., Abdullah, S. N., Brza, M. A. *Polymers*, 2020, **12**, 2627.
2. Zhang, Z., Liao, M., Lou, H., Hu, Y., Sun, X., Peng, H. *Adv. Mater.*, 2018, **30**, 1704261.
3. Neo, W. T., Ye, Q., Chua, S.-J., Xu, J. *J. Mater. Chem. C*, 2016, **4**, 7364–7376.
4. Li, X., Perera, K., He, J., Gumyusenge, A., Mei, J. *J. Mater. Chem. C*, 2019, **7**, 12761–12789.
5. Borges-González, J., Kousseff, C. J., Nielsen, C. B. *J. Mater. Chem. C*, 2019, **7**, 1111–1130.
6. Wang, Y., Zhu, C., Pfattner, R., Yan, H., Jin, L., Chen, S., Molina-Lopez, F., Lissel, F., Liu, J., Rabiah, N. I., Chen, Z., Chung, J. W., Linder, C., Toney, M. F., Murmann, B., Bao, Z. *Sci. Adv.*, 2017, **3**, e1602076.
7. Walczak, R. M., Reynolds, J. R. *Adv. Mater.*, 2006, **18**, 1121–1131.
8. Heywang, G., Jonas, F. *Adv. Mater.*, 1992, **4**, 116–118.
9. Wustoni, S., Hidalgo, T. C., Hama, A., Ohayon, D., Savva, A. *Adv. Mater. Technol.*, 2019, 1900943.
10. Berggren, M., Richter-Dahlfors, A. *Adv. Mater.*, 2007, **19**, 3201–3213.
11. Liao, J., Si, H., Zhang, X., Lin, S. *Sensors*, 2019, **19**, 218.
12. Zainal, M. F., Mohd, Y. *Polym. - Plast. Technol. Eng.*, 2015, **54**, 276–281.
13. Xie, K., Glasser, A., Shinde, S., Zhang, Z., Rampnoux, J.-M., Maali, A., Cloutet, E., Hadziioannou, G., Kellay, H. *Adv. Funct. Mater.*, 2021, **31**, 2009039.
14. Cui, X. T., Zhou, D. D. *IEEE Trans. Neural Syst. Rehabil. Eng.*, 2007, **15**, 502–508.
15. Reddy, S., Xiao, Q., Liu, H., Li, C., Chen, S., Wang, C., Chiu, K., Chen, N., Tu, Y., Ramakrishna, S., He, L. *ACS Appl. Mater. Interfaces*, 2019, **11**, 18254–18267.
16. Donahue, M. J., Sanchez-Sanchez, A., Inal, S., Qu, J., Owens, R. M., Mecerreyes, D.,

Malliaras, G. G., Martin, D. C. *Mater. Sci. Eng. R Reports*, 2020, **140**, 100546.

17. Nikiforidis, G., Wustoni, S., Routier, C., Hama, A., Koklu, A., Saleh, A., Steiner, N., Druet, V., Fiumelli, H., Inal, S. *Macromol. Biosci.*, 2020, **20**, 2000215.
18. Wei, B., Liu, J., Ouyang, L., Kuo, C. C., Martin, D. C. *ACS Appl. Mater. Interfaces*, 2015, **7**, 15388–15394.
19. Poverenov, E., Li, M., Bitler, A., Bendikov, M. *Chem. Mater.*, 2010, **22**, 4019–4025.
20. Bhagwat, N., Kiick, K. L., Martin, D. C. *J. Mater. Res.*, 2014, **29**, 2835–2844.
21. Groenendaal, L. B., Jonas, F., Freitag, D., Pielartzik, H., Reynolds, J. R. *Adv. Mater.*, 2000, **12**, 481–494.
22. Bu, H.-B., Götz, G., Reinold, E., Vogt, A., Schmid, S., Blanco, R., Segura, J. L., Bäuerle, P. *Chem. Commun.*, 2008, 1320–1322.
23. Kumar, A., Welsh, D. M., Morvant, M. C., Piroux, F., Abboud, K. A., Reynolds, J. R. *Chem. Mater.*, 1998, **10**, 896–902.
24. Gaupp, C. L., Welsh, D. M., Reynolds, J. R. *Macromol. Rapid Commun.*, 2002, **23**, 885–889.
25. Roquet, S., Leriche, P., Perepichka, I., Jousselme, B., Levillain, E., Frère, P., Roncali, J. *J. Mater. Chem.*, 2004, **14**, 1396–1400.
26. Sassi, M., Mascheroni, L., Ruffo, R., Salamone, M. M., Pagani, G. A., Mari, C. M., D'Orazio, G., La Ferla, B., Beverina, L. *Org. Lett.*, 2013, **15**, 3502–3505.
27. Povlich, L. K., Cheol, J., Leach, M. K., Corey, J. M., Kim, J., Martin, D. C. *Biochim. Biophys. Acta*, 2013, **1830**, 4288–4293.
28. Mantione, D., Marquez, A. V., Cruciani, F., Brochon, C., Cloutet, E., Hadziioannou, G. *ACS Macro Lett.*, 2019, **8**, 285–288.
29. Ali, E. M., Kantchev, E. A. B., Yu, H. H., Ying, J. Y. *Macromolecules*, 2007, **40**, 6025–6027.
30. Godeau, G., N'Na, J., El Kout, E., Ben Trad, R., Darmanin, T., El Kateb, M., Beji, M.,

Guittard, F. *Polym. Adv. Technol.*, 2016, **27**, 993–998.

31. Casado, N., Hernández, G., Veloso, A., Devaraj, S., Mecerreyes, D., Armand, M. *ACS Macro Lett.*, 2016, **5**, 59–64.
32. Sankaran, B., Reynolds, J. R. *Macromolecules*, 1997, **30**, 2582–2588.
33. Zhang, S., Xu, J., Lu, B., Qin, L., Zhang, L., Zhen, S., Mo, D. *J. Polym. Sci. Part A Polym. Chem.*, 2014, **52**, 1989–1999.
34. Hu, D., Lu, B., Duan, X., Xu, J., Zhang, L., Zhang, K., Zhang, S., Zhen, S. *RSC Adv.*, 2014, **4**, 35597–35608.
35. Dong, L., Zhang, Y., Duan, X., Zhu, X., Sun, H., Xu, J. *Anal. Chem.*, 2017, **89**, 9695–9702.
36. Salinas, G., Villarroel Marquez, A., Idir, M., Shinde, S., Frontana-Uribe, B. A., Raoux, M., Lang, J., Cloutet, E., Kuhn, A. *ChemElectroChem*, 2020, **7**, 2826–2830.
37. Trippé, G., Le Derf, F., Lyskawa, J., Mazari, M., Roncali, J., Gorgues, A., Levillain, E., Sallé, M. *Chem. - A Eur. J.*, 2004, **10**, 6497–6509.
38. Rodríguez-Jiménez, S., Bennington, M. S., Akbarinejad, A., Tay, E. J., Chan, E. W. C., Wan, Z., Abudayyeh, A. M., Baek, P., Feltham, H. L. C., Barker, D., Gordon, K. C., Travas-Sejdic, J., Brooker, S. *ACS Appl. Mater. Interfaces*, 2021, **13**, 1301–1313.
39. Kannan, B., Williams, D. E., Laslau, C., Travas-Sejdic, J. *Biosens. Bioelectron.*, 2012, **35**, 258–264.
40. Savagian, L. R., Österholm, A. M., Ponder, J. F., Barth, K. J., Rivnay, J., Reynolds, J. R. *Adv. Mater.*, 2018, **30**, 1804647.
41. Jones, A. L., De Keersmaecker, M., Savagian, L. R., DiTullio, B. T., Pelse, I., Reynolds, J. R. *Adv. Funct. Mater.*, 2021, 2102688.
42. Parr, Z. S., Nielsen, C. B. *Mater. Chem. Front.*, 2020, **4**, 2370–2377.
43. Wustoni, S., Combe, C., Ohayon, D., Akhtar, M. H., McCulloch, I., Inal, S. *Adv. Funct. Mater.*, 2019, **29**, 1904403.

44. Burés, J., Martín, M., Urpí, F., Vilarrasa, J. *J. Org. Chem.*, 2009, **74**, 2203–2206.

45. Segura, J. L., Gómez, R., Reinold, E., Bäuerle, P. *Org. Lett.*, 2005, **7**, 2345–2348.

46. Surya, S. G., Raval, H. N., Ahmad, R., Sonar, P., Salama, K. N., Rao, V. R. *Trends Anal. Chem.*, 2018, **111**, 27–36.

47. Levasseur, D., Mjejri, I., Rolland, T., Rougier, A. *Polymers*, 2019, **11**, 179.

48. Volkov, A. V., Wijeratne, K., Mitraka, E., Ail, U., Zhao, D., Tybrandt, K., Andreasen, J. W., Berggren, M., Crispin, X., Zozoulenko, I. V. *Adv. Funct. Mater.*, 2017, **27**, 1700329.

49. Sahalianov, I., Singh, S. K., Tybrandt, K., Berggren, M., Zozoulenko, I. *RSC Adv.*, 2019, **9**, 42498–42508.

50. Berggren, M., Malliaras, G. G. *Science*, 2019, **364**, 233–234.

51. Gueye, M. N., Carella, A., Faure-Vincent, J., Demadrille, R., Simonato, J.-P. *Prog. Mater. Sci.*, 2020, **108**, 100616.

52. Yamamoto, J., Furukawa, Y. *J. Phys. Chem. B*, 2015, **119**, 4788–4794.

53. Voss, M. G., Scholes, D. T., Challa, J. R., Schwartz, B. J. *Faraday Discuss.*, 2019, **216**, 339–362.

54. Voss, M. G., Challa, J. R., Scholes, D. T., Yee, P. Y., Wu, E. C., Liu, X., Park, S. J., León Ruiz, O., Subramaniyan, S., Chen, M., Jenekhe, S. A., Wang, X., Tolbert, S. H., Schwartz, B. J. *Adv. Mater.*, 2021, **33**, 2000228.

55. Spano, F. C. *Acc. Chem. Res.*, 2010, **43**, 429–439.

56. Finn, P. A., Jacobs, I. E., Armitage, J., Wu, R., Paulsen, B. D., Freeley, M., Palma, M., Rivnay, J., Sirringhaus, H., Nielsen, C. B. *J. Mater. Chem. C*, 2020, **8**, 16216–16223.

57. Carli, S., Casarin, L., Bergamini, G., Caramori, S., Bignozzi, C. A. *J. Phys. Chem. C*, 2014, **118**, 16782–16790.

58. Ouyang, L., Wei, B., Kuo, C., Pathak, S., Farrell, B., Martin, D. C. *Sci. Adv.*, 2017, **3**, e1600448.

59. Villemin, E., Lemarque, B., Vũ, T. T., Nguyen, V. Q., Trippé-Allard, G., Martin, P., Lacaze, P.-C., Lacroix, J.-C. *Synth. Met.*, 2019, **248**, 45–52.

60. Gaupp, C. L., Welsh, D. M., Rauh, R. D., Reynolds, J. R. *Chem. Mater.*, 2002, **14**, 3964–3970.

61. Daugaard, A. E., Hvilsted, S., Hansen, T. S., Larsen, N. B. *Macromolecules*, 2008, **41**, 4321–4327.

C. J. Kousseff, F. E. Taifakou, W. G. Neal, M. Palma, C. B. Nielsen*

Controlling morphology, adhesion and electrochromic behavior of PEDOT films through molecular design and processing

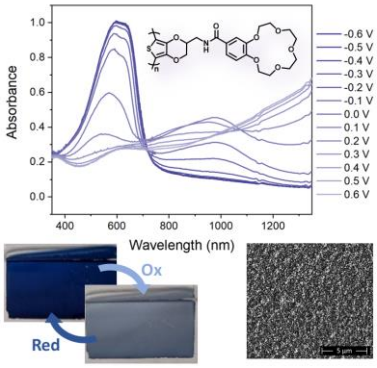

Supporting Information

Controlling morphology, adhesion and electrochromic behavior of PEDOT films through molecular design and processing

*Christina J. Kousseff, Fani Eirini Taifakou, William G. Neal, Matteo Palma, Christian B. Nielsen**

List of figures

S1. Investigating PEDOT morphology

In this section, an in-depth investigation into the optimal parameters for film deposition by either chronoamperometry or cyclic voltammetry is conducted. All films in this section are electropolymerized from 3,4-ethylenedioxythiophene (EDOT) monomer solution alongside 0.1 M $NaClO_4$ as the supporting electrolyte in degassed acetonitrile; for cyclic voltammetry, a voltage range of -0.5 – +1.2 V was applied; all films are deposited on indium tin oxide (ITO) coated glass slides. Other variables are specified within each experiment below, and resulting films were analyzed with a surface profilometer and by optical microscopy.

S1.1. Films made by cyclic voltammetry

S1.1.1. Number of scans and monomer concentration

The variable with the largest impact on film thickness in cyclic voltammetry was found to be the number of scans; starting with 10 mM monomer solution and 50 mV/s scan rate, initial measurements taken at 10-scan intervals up to 30 scans resulted in a steep linear increase of film thickness from 1 µm (10 scans) to 5 µm (30 scans), after which point, the surface profile for films made from 40 scans could not be measured due to the extent of wrinkling, poor adhesion and delamination caused by the extreme thickness of the film produced. Because of this, scan number experiments were conducted in tandem with the variation of monomer concentration; in general, for concentrations 1.25 mM, 2.5 mM, 5 mM, and 10 mM, film thickness also increased linearly with number of scans. The results in **Figure S1a** illustrate the relationship between number of scans, concentration and thickness; it is shown that reducing monomer concentration decreases the gradient of the scan number/thickness relationship: the difference in thickness between monomer concentrations is negligible at 10 scans with all films <1 µm in thickness, but becomes increasingly pronounced at higher scan numbers, with films too thick to analyze or apply in a device. Therefore, 10 scans is chosen as an appropriate measure for future film depositions.

S1.1.2. Scan rate

As shown in **Figure S1b,** scan rate has an inverse relationship to film thickness. Due to the exponentially thicker films that are produced at lower scan rates, a monomer concentration of 2.5 mM was used to ensure a full data set representative of this trend could be obtained. It is observed that while scan rates up to and including 50 mV/s produce good quality films, they are far too thick (approaching and above 1 μm) to be useful for device applications; however, at the fastest tested scan rate (200 mV/s), films are of poor quality, with surface defects visible to the naked eye. Therefore, a rate of 100 mV/s produces films with the best compromise between these adverse properties.

S1.2. Films made by chronoamperometry

S1.2.1. Potential

The choice of applied potential in chronoamperometry is crucial. As potentiostatic polymerization produces thinner films in general than cyclic voltammetry, a 10 mM concentration of EDOT was used. Four potentials, +0.8 V, +1.2 V, +1.6 V, and +2.0 V were applied for 45 sec: as shown in **Figure S1c,** at +0.8 V, which is below the oxidation potential of the EDOT monomer (+1.0 V), no polymer film was formed. Above this potential, film thickness is variable, with a local peak at +1.2 V (0.4 μm), subsequently decreasing at +1.6 V. At +2.0 V (0.5 μm), although a thicker film was made, a purple coloration of the film was observed, alongside leaching of the polymeric material from the substrate, suggesting overoxidation resulting in material degradation.

S1.2.2. Deposition time

Finally, the amount of time for which the potential is applied in chronoamperometry has a demonstrable effect on film thickness. Using the optimal potential above of +1.2 V, with a 10 mM concentration of EDOT, films were deposited for time frames between 12.5 – 180 sec. **Figure S1d** shows the results of this, in which thickness increases with time. Within these

parameters, the optimal time for deposition is 45 seconds, as it produces films of approximately 0.5 µm, within the previously specified ideal range.

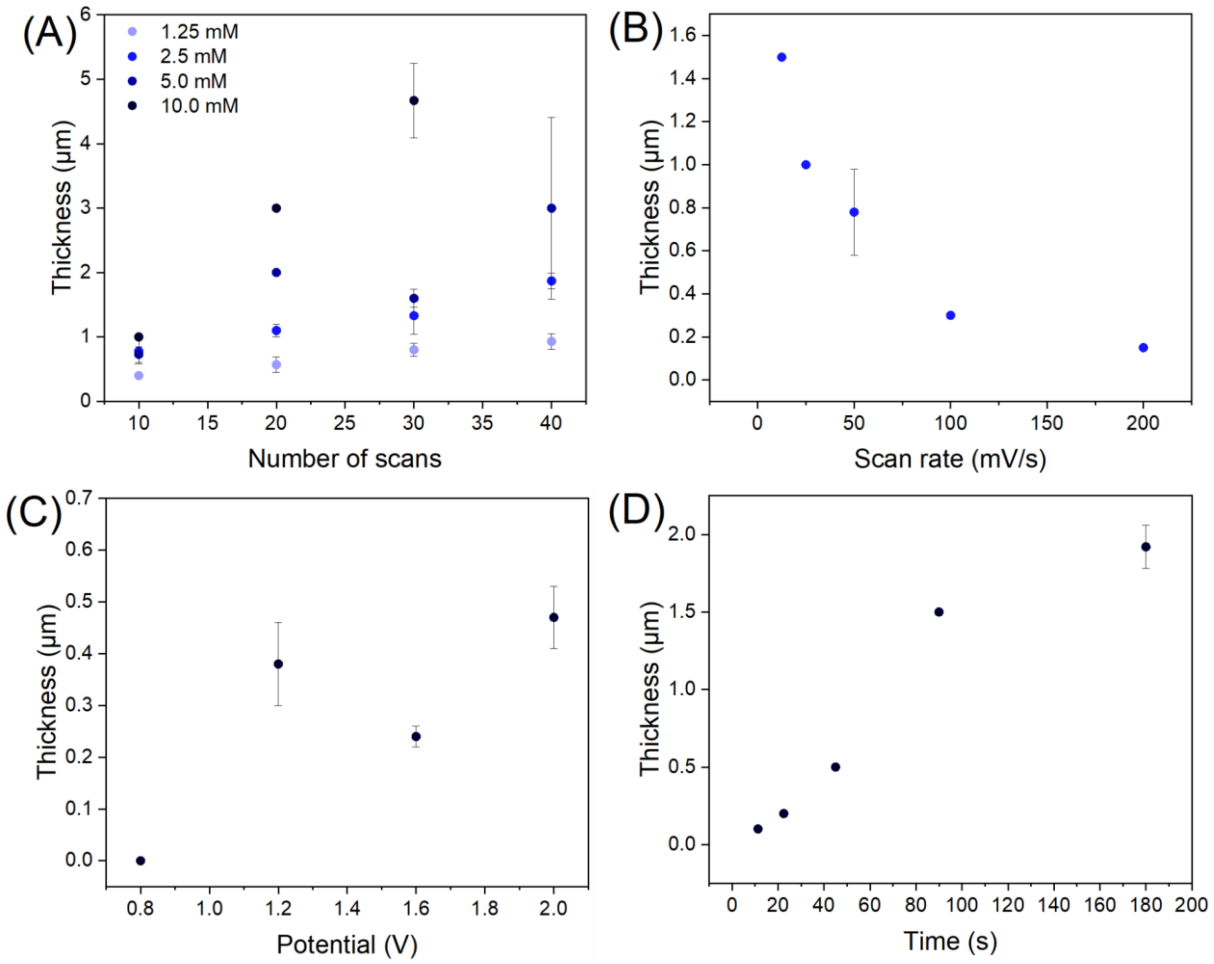

Figure S1. Relationships between **PEDOT** film thickness and a) monomer concentration and number of scans in cyclic voltammetry; b) scan rate in cyclic voltammetry (monomer concentration 2.5 mM); c) applied potential in chronoamperometry (monomer concentration 10 mM); d) deposition time in chronoamperometry (applied potential of +1.2 V, monomer concentration 10 mM). All experiments carried out in degassed acetonitrile with 0.1 M $NaClO_4$ as the supporting electrolyte. Thicknesses are given as the average of three measurements and error bars represent the standard deviation between these values.

S1.3. Roughness and wrinkling

Combining the results of these investigations, the selected parameters for optimal **PEDOT** film thickness within this work can be summarized as: 10 scans from -0.5 to +1.2 V at 0.1 V/s for potentiodynamic electropolymerization, and +1.2 V for 45 sec for potentiostatic electropolymerization, both with 10 mM monomer concentration. However, it is not only thickness that must be considered; error bars in **Figure S1a-d** representing the standard deviation of film thicknessess points towards a general trend that thicker films, especially those made by cyclic voltammetry, show decreased uniformity compared to thinner films. Inspection of these films under an optical microscope (**Figure S2**) reveals film wrinkling due to poor adhesion to the substrate surface.[1,2]

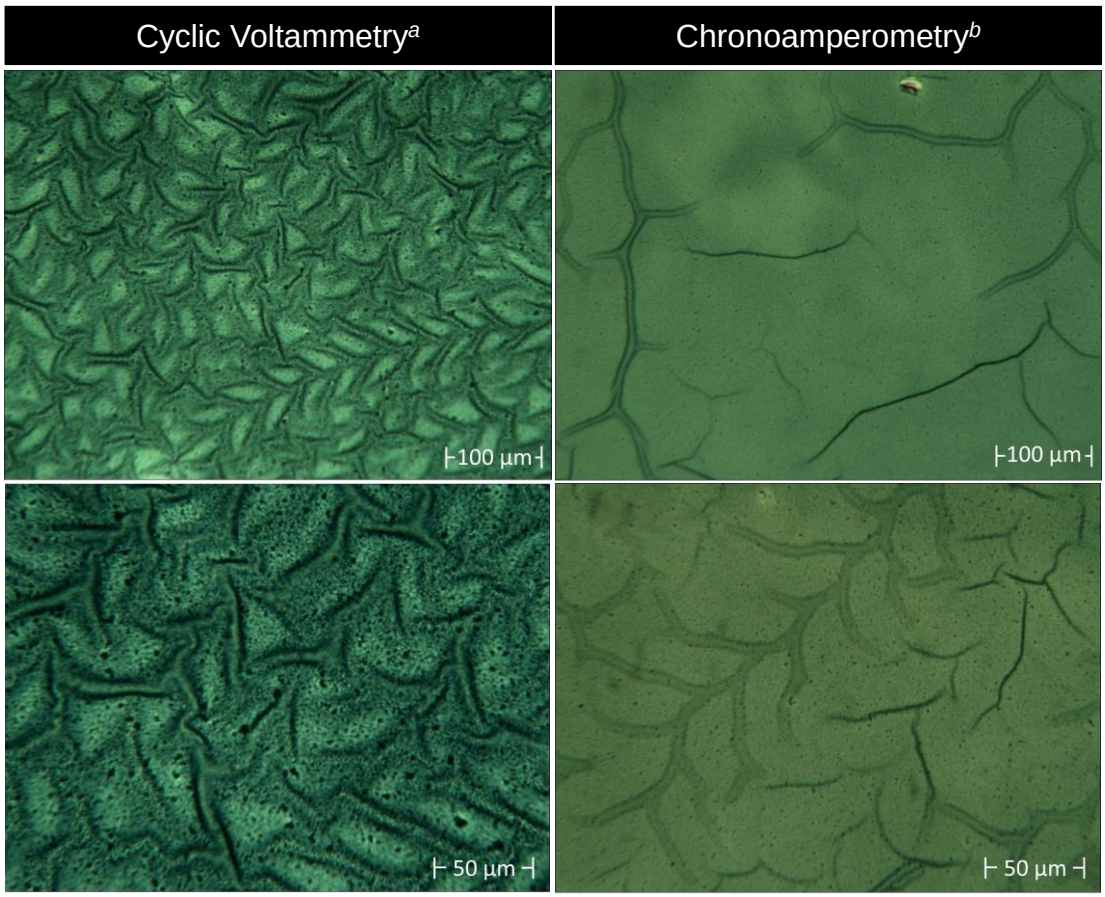

Figure S2. Optical microscope images of **PEDOT** on ITO-coated glass substrates after deposition by a) cyclic voltammetry (-0.5 – +1.2 V, 10 scans, 10 mM EDOT, 100 mV/s); and b) chronoamperometry (+1.2 V, 45 sec, 10 mM EDOT).

Spectroelectrochemistry (isosbestic points) of PEDOT and PEDOT-Crown

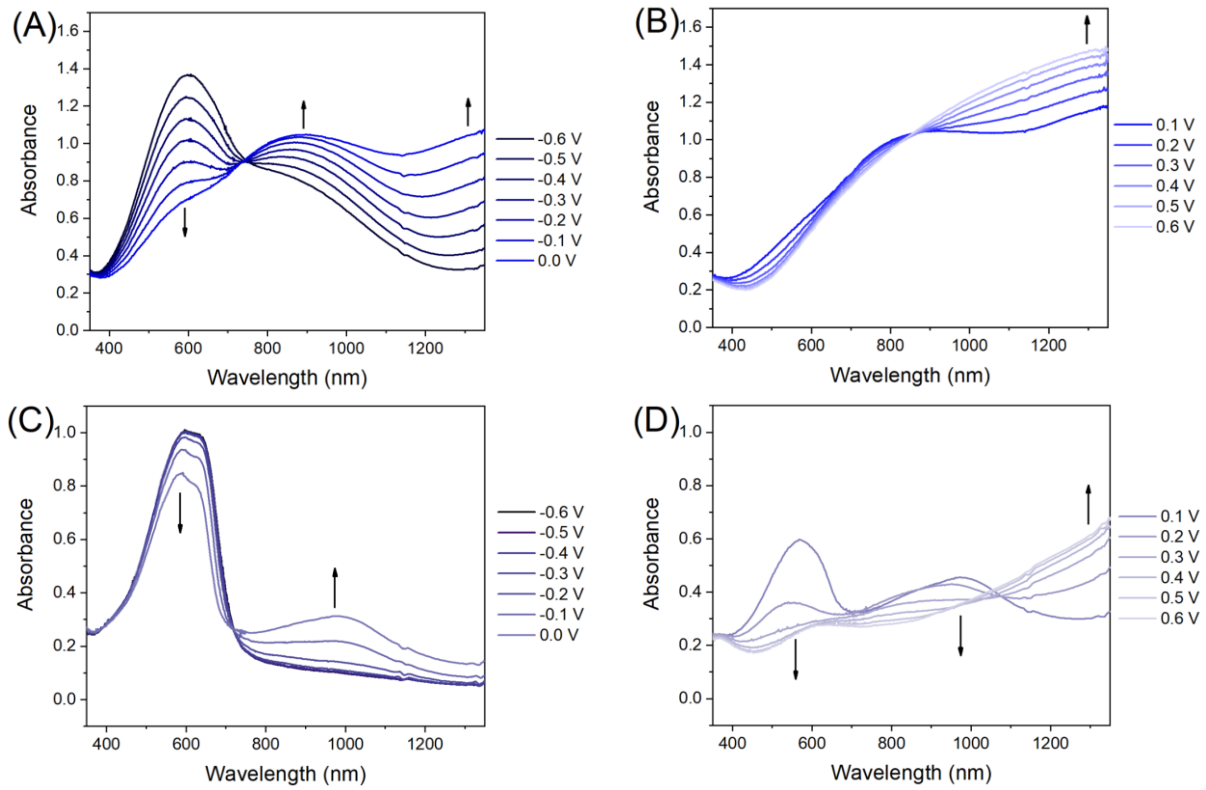

Figure S3. Spectroelectrochemical analysis of polymers a) **PEDOT** in 0.1 M $NaClO_4$ in H_2O in the range -0.6 V to 0.0 V, showing concurrent formation of the polaron and bipolaron; b) **PEDOT** in 0.1 M $NaClO_4$ in H_2O in the range +0.1 V to +0.6 V, showing bipolaron formation; c) **PEDOT-Crown** in 0.1 M $NaClO_4$ in H_2O in the range -0.6 V to 0.0 V, showing formation of the polaron only; d) **PEDOT-Crown** in 0.1 M $NaClO_4$ in H_2O in the range +0.1 to +0.6 V, showing simultaneous polaron depletion and bipolaron formation. Arrows depict the increase or decrease of peaks corresponding to the increasing applied voltage within each given range.

Bleaching of neutral absorption band

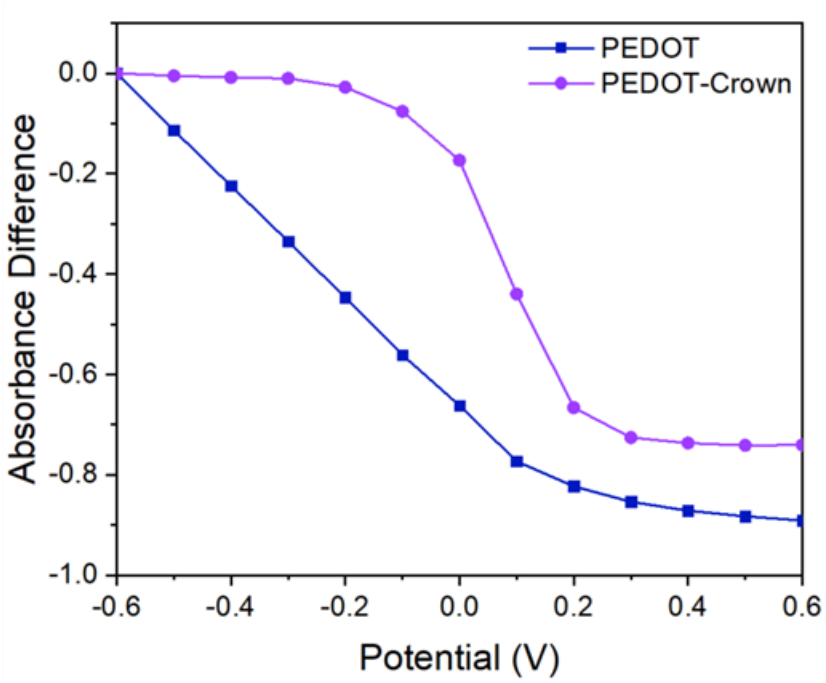

Figure S4. Bleaching (absorbance difference from neutral spectrum at -0.6 V) plotted *vs.* applied potential for **PEDOT** (recorded at 570 nm) and **PEDOT-Crown** (recorded at 596 nm)

Cycling stability of PEDOT and PEDOT-Crown in 1X PBS

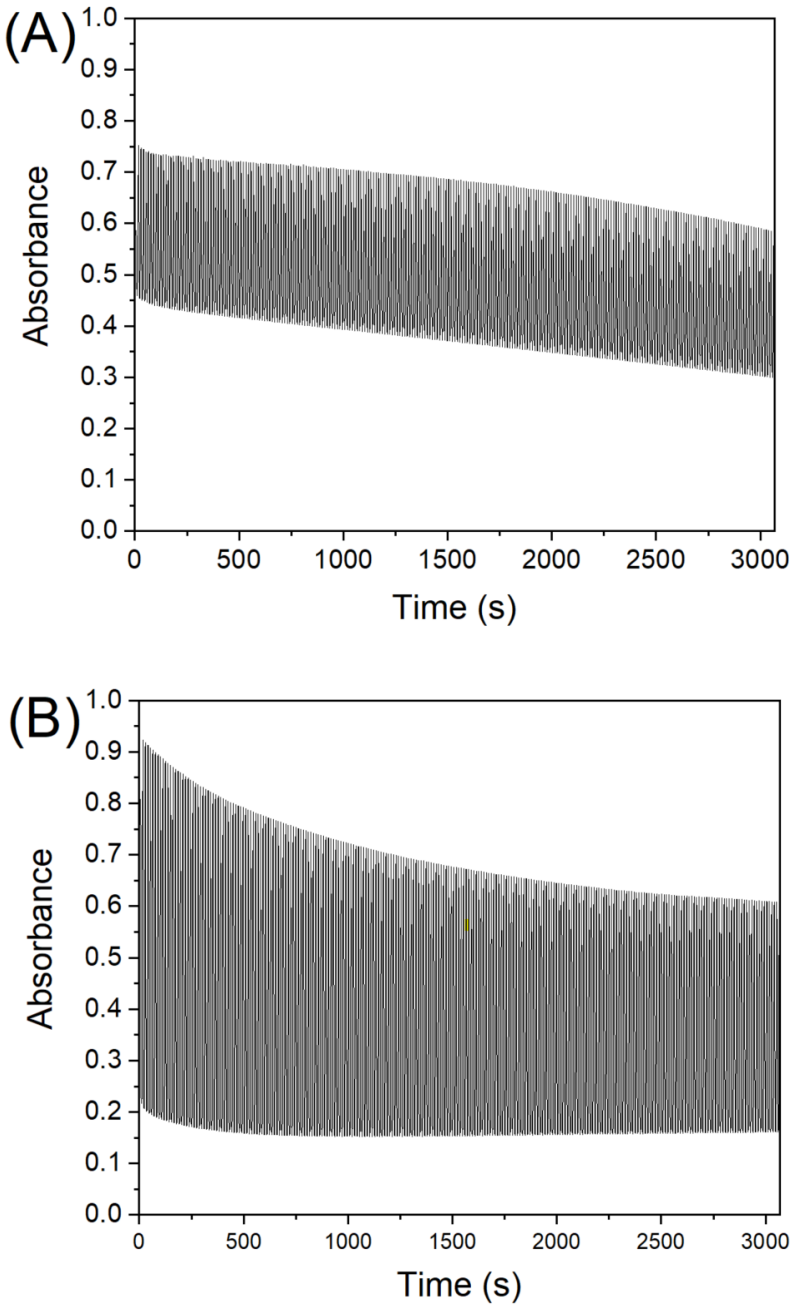

Figure S5. Cycling stability in 1X PBS (pH 7.4) over 205 cycling voltammetry scans (-0.6 – +1.2 V) for a) **PEDOT** (λ_{max} = 600 nm), and b) **PEDOT-Crown** (λ_{max} = 575 nm) deposited by chronoamperometry (+1.2 V, 45 sec, 10 mM monomer) on ITO-glass.

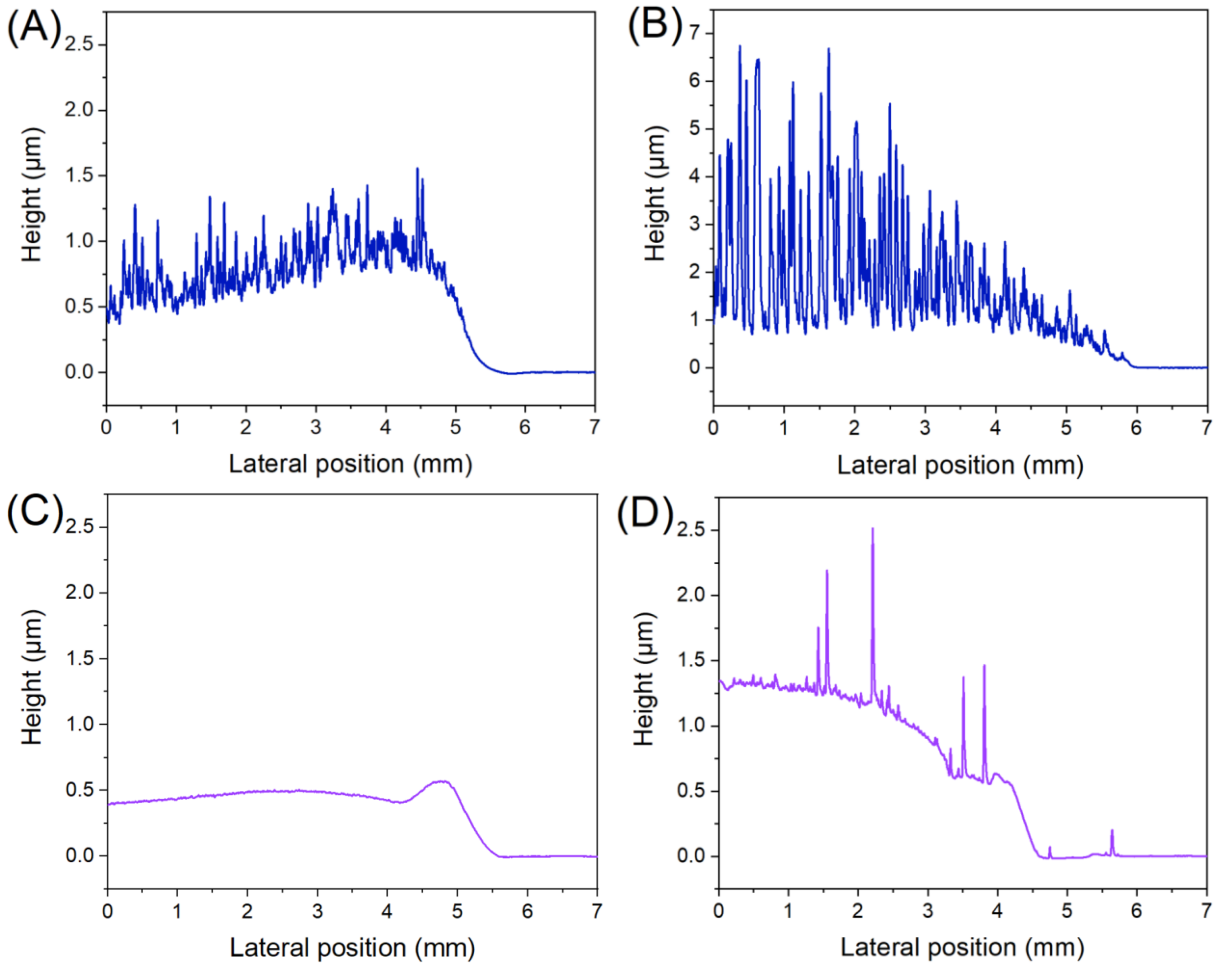

Figure S6. Example surface profiles of a) **PEDOT** deposited by chronoamperometry; b) **PEDOT** deposited by cyclic voltammetry; c) **PEDOT-Crown** deposited by chronoamperometry; d) **PEDOT-Crown** deposited by cyclic voltammetry. Chronoamperometry (+1.2 V for 45 sec) and cyclic voltammetry (10 cycles from -0.5 V to +1.2 V, 0.1 V/s) performed in 0.1 M $TBAClO_4$ in acetonitrile with 10 mM monomer.

AFM images normalized to comparative scales

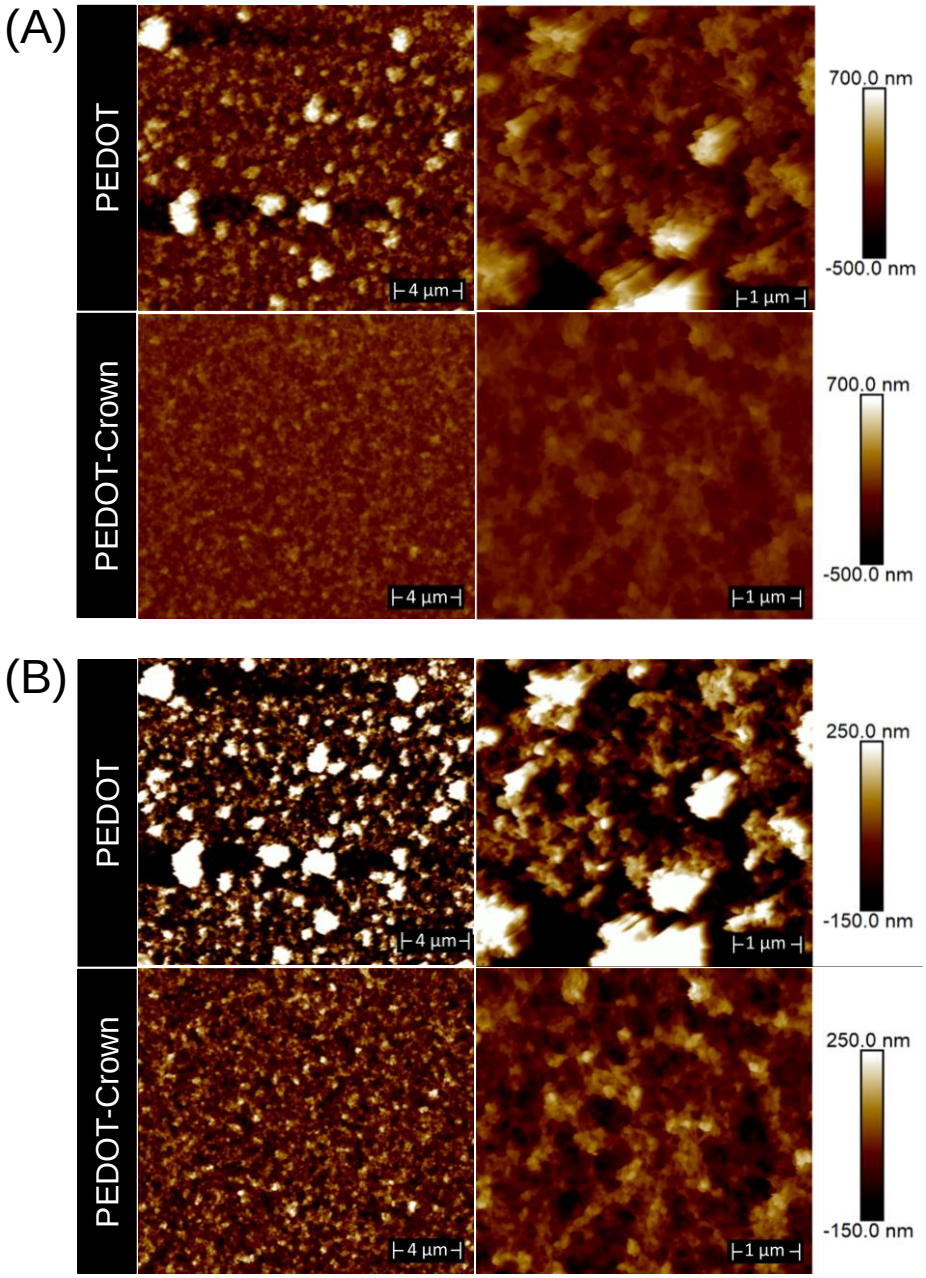

Figure S7. AFM images of **PEDOT and PEDOT-Crown** polymers with comparable depth scales normalized appropriate to a) **PEDOT** (-500 nm to 700 nm) and b) **PEDOT-Crown** (-150 nm to 250 nm)

Electrochromic switching of PEDOT in the range -0.6 V to 0.5 V

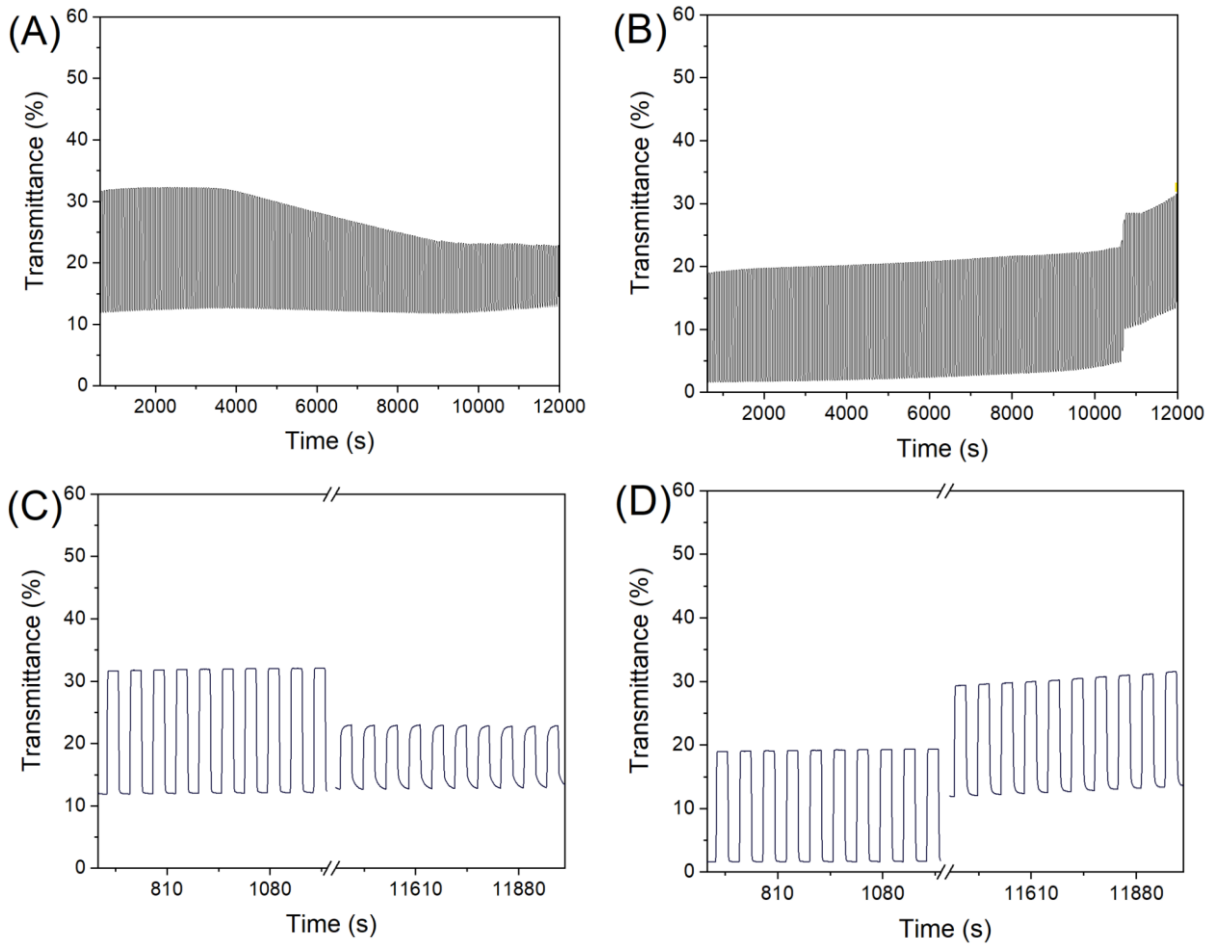

Figure S8. Cycles 11-200 electrochromic switching between -0.6 V – +0.5 V for a) **PEDOT** with 0.1 M $TBAClO_4$ in MeCN b) **PEDOT** with 0.1 M $NaClO_4$ in H_2O; and close up of electrochromic switching cycles 11-20 (initial) vs.191-200 (last) between -0.6 V – +0.5 V for c) **PEDOT** with 0.1 M $TBAClO_4$ in MeCN d) **PEDOT** with 0.1 M $NaClO_4$ in H_2O (the abrupt increase in T% around 10600 seconds, cycle 176 we suspect represents a delamination event, as the film was partially delaminated upon inspection at the end of the experiment)

NMR Spectra for 2-(chloromethyl)-2,3-dihydrothieno[3,4-*b*][1,4]dioxine (EDOT-Cl)

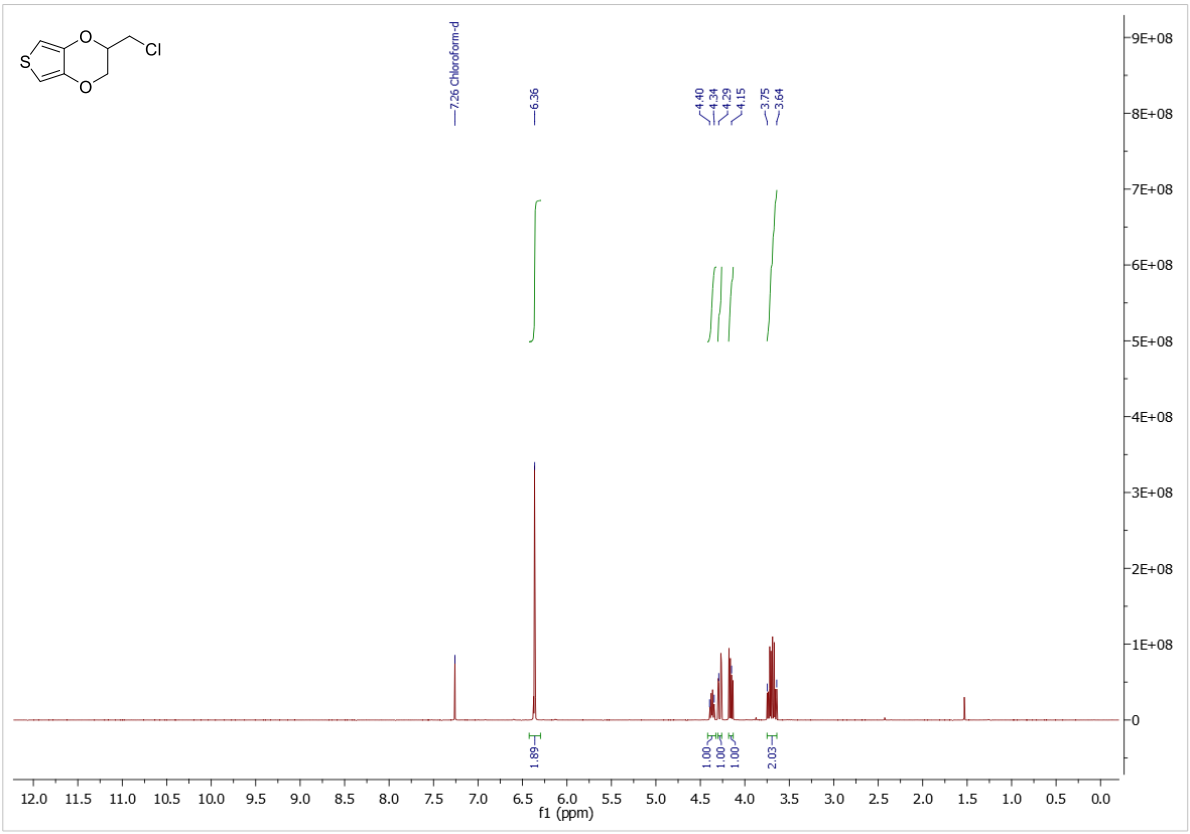

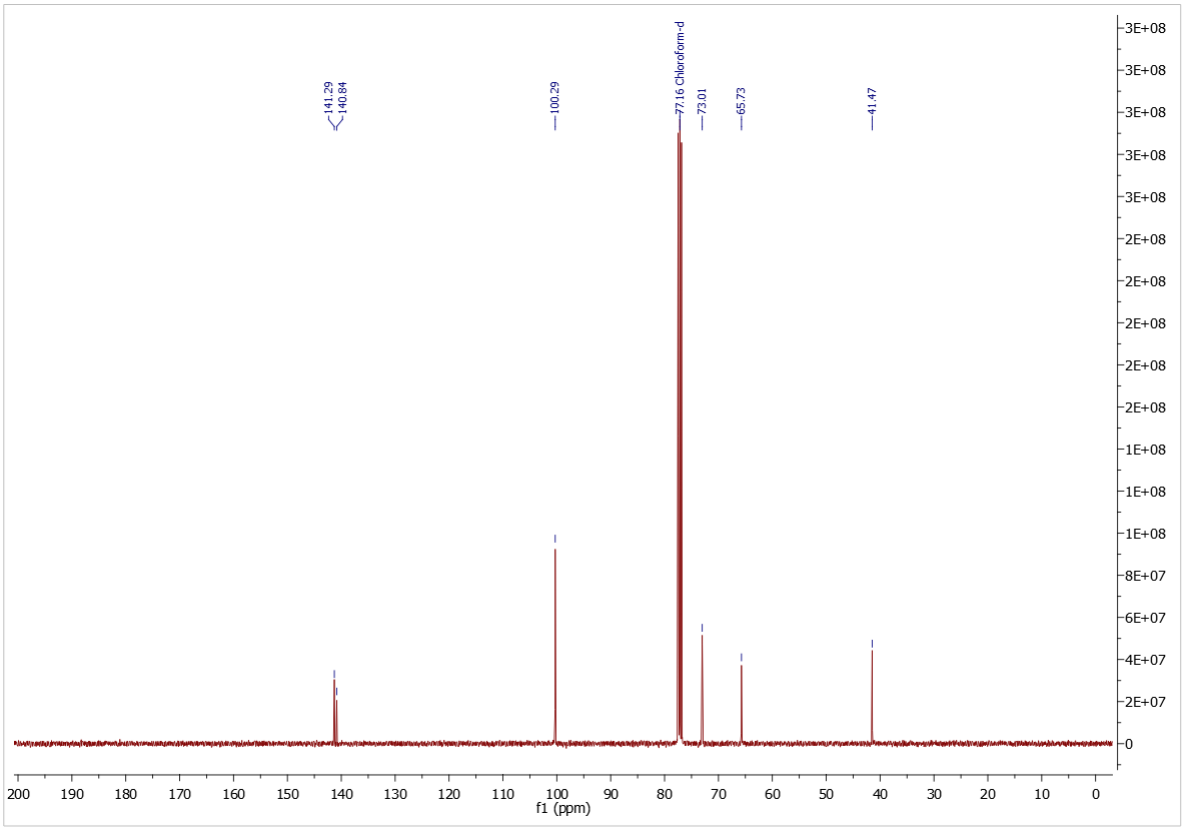

NMR Spectra for 2-(azidomethyl)-2,3-dihydrothieno[3,4-*b*][1,4]dioxine (EDOT-N_3)

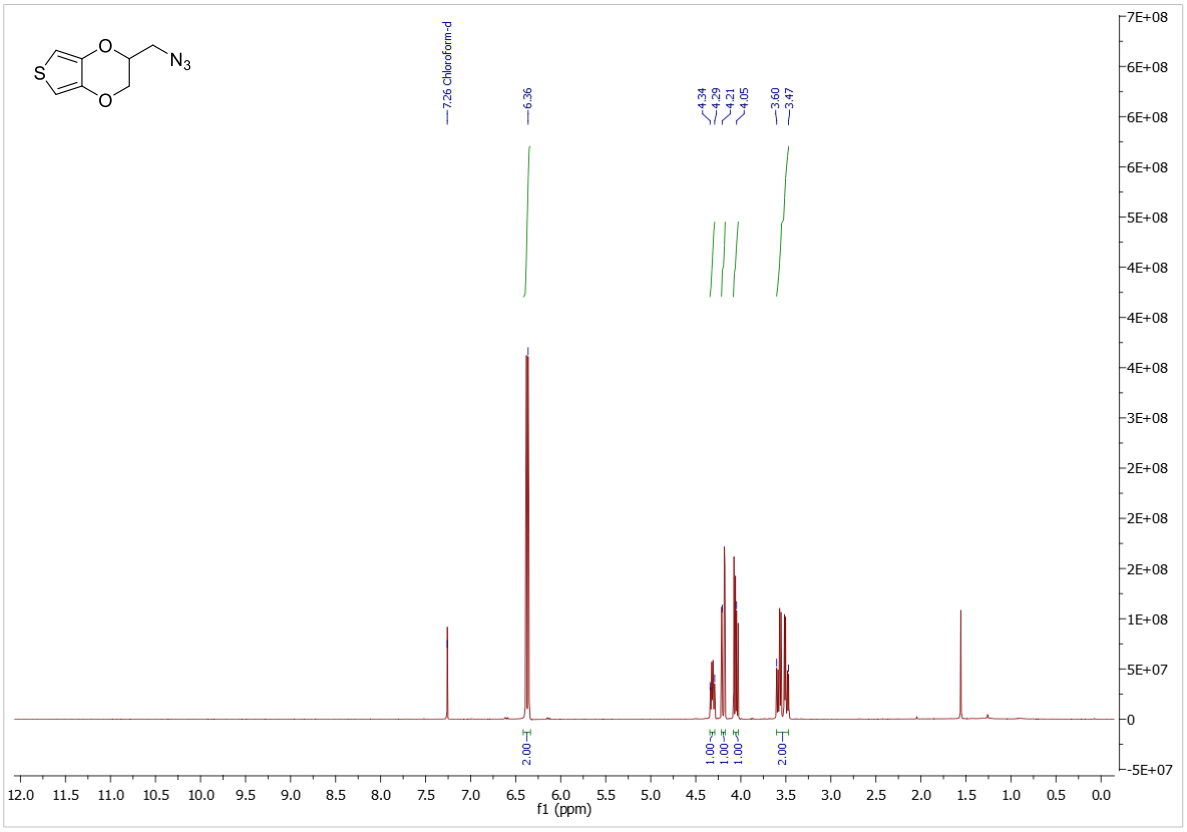

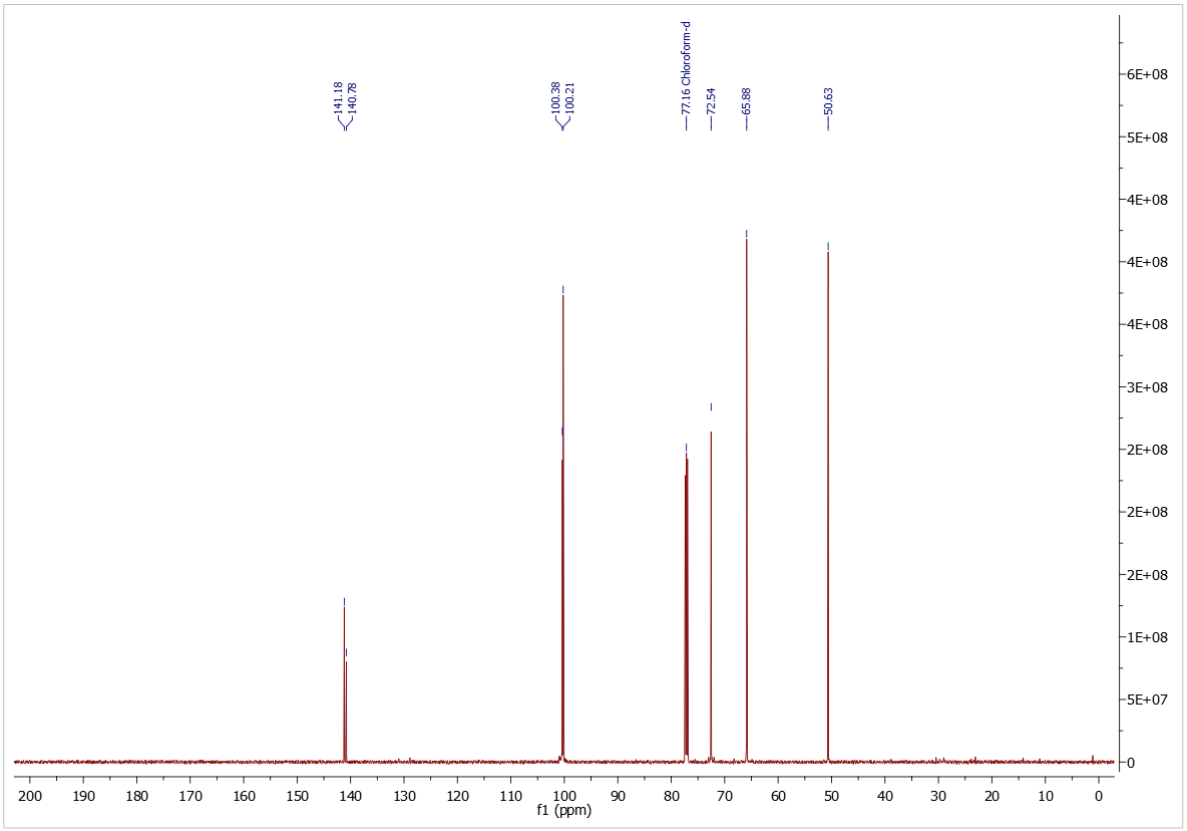

NMR Spectra for *N*-((2,3-dihydrothieno[3,4-*b*][1,4]dioxin-2-yl)methyl)-2,3,5,6,8,9,11,12-octahydrobenzo[*b*][1,4,7,10,13]pentaoxacyclopentadecine-15-carboxamide (EDOT-Crown)

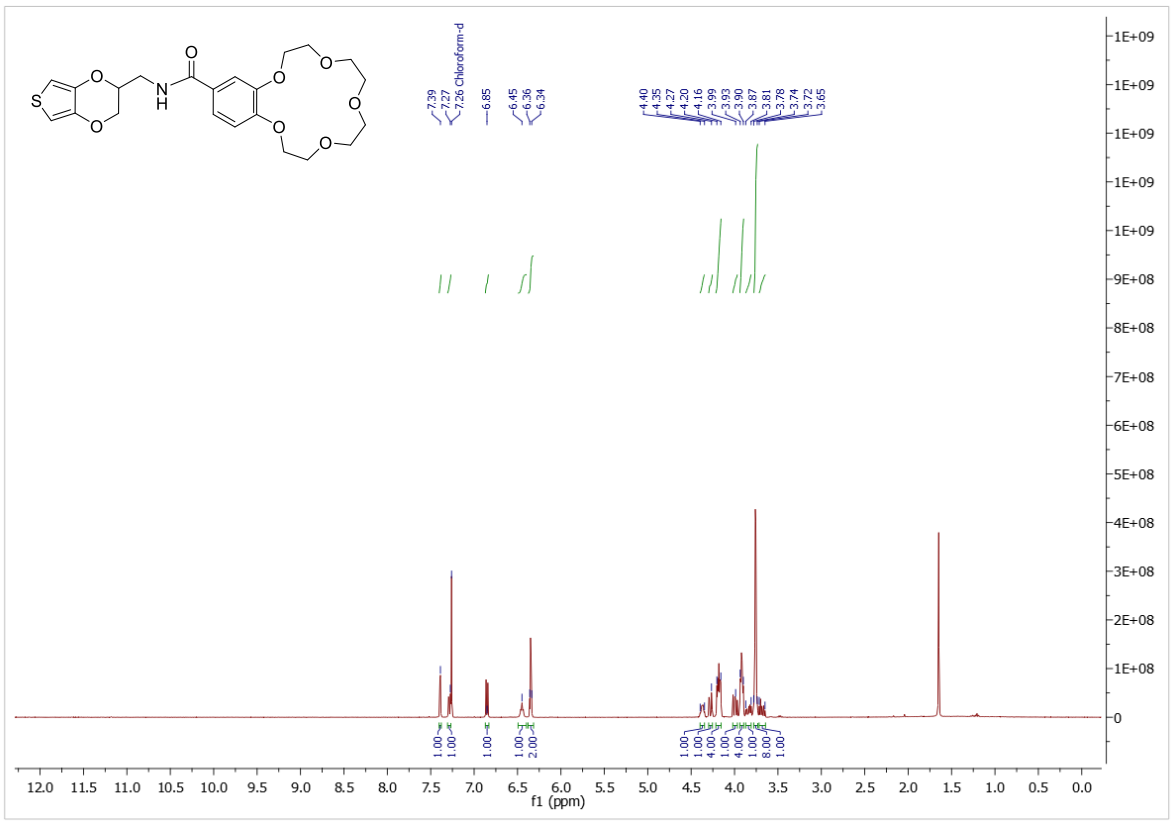

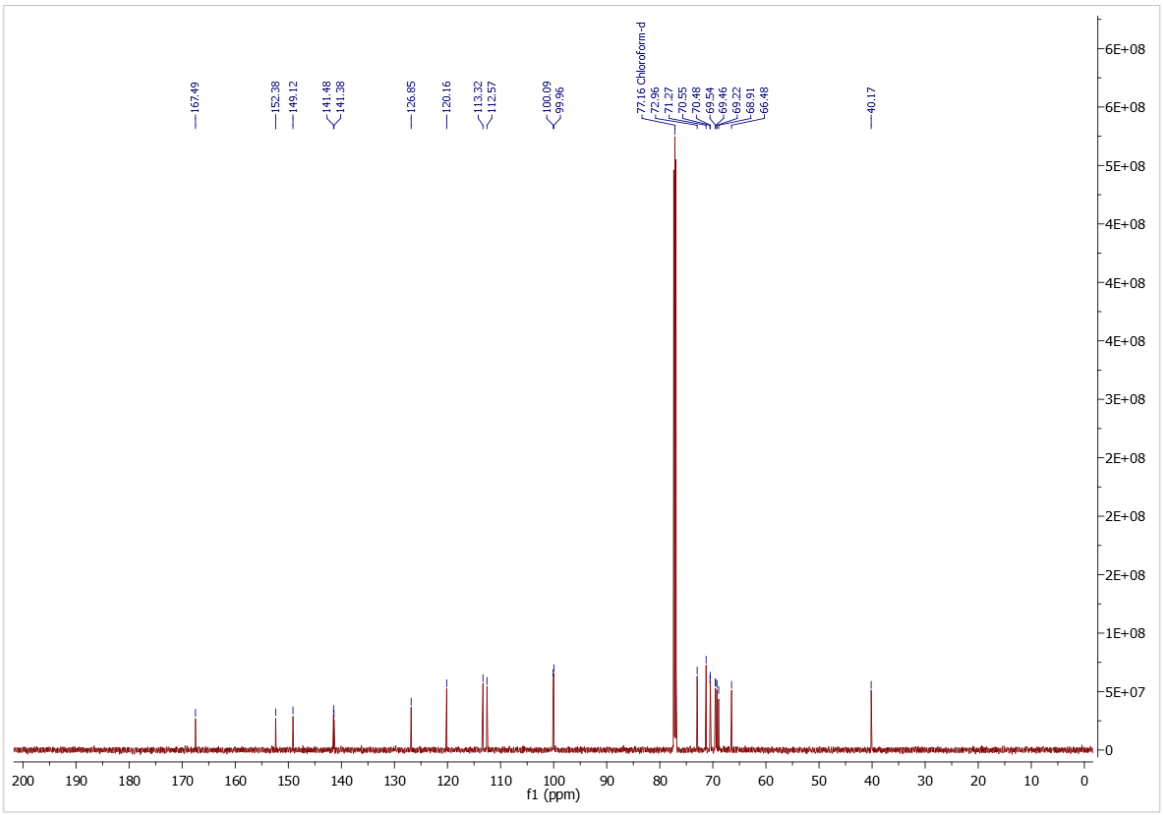

References

1. Xie, K., Glasser, A., Shinde, S., Zhang, Z., Rampnoux, J.-M., Maali, A., Cloutet, E., Hadziioannou, G., Kellay, H. *Adv. Funct. Mater.*, 2021, **31**, 2009039.
2. Poverenov, E., Li, M., Bitler, A., Bendikov, M. *Chem. Mater.*, 2010, **22**, 4019–4025.